Diffusion-Bonded Nonlinear Materials for Practical Quasi-Phase-Matched Mid-IR Devices

Final Technical Report
Office of Naval Research
Grant N00014-94-1-0426
December 1, 1993 through September 30, 1995

Robert L. Byer
Principal Investigator

Ginzton Laboratory Report No. 5409
April 1996

Edward L. Ginzton Laboratory
Stanford University
Stanford, California 94305-4085

Diffusion-Bonded Nonlinear Materials for Practical Quasi-Phase-Matched Mid-IR Devices

ONR Grant N00014-94-1-0426
Final Technical Report

Robert L. Byer
Edward L. Ginzton Laboratory
Stanford University
Stanford, California 94305-4085

ABSTRACT

This report summarizes research on the application of diffusion-bonded GaAs for high power quasi-phasematched nonlinear frequency conversion in the infrared (IR). Research focused on development of material processing methods. Microstructural, microchemical and optical characterization techniques were employed to analyze the nature of defects found at the wafer interfaces, and within the bulk material; strategies for minimizing them were developed. The resulting advances in processing technology reduced mid-IR optical losses in diffusion-bonded GaAs stacks by over an order of magnitude, to less than 0.2% per interface. This is within the range required to make practical pulsed nonlinear infrared devices such as CO_2 doublers. Further reductions in optical losses, required for high average power cw IR applications, appear possible.

Diffusion-Bonded Nonlinear Materials for Practical Quasi-Phase-Matched Mid-IR Devices

ONR Grant N00014-94-1-0426
Final Technical Report

Table of Contents

Diffusion-Bonded Nonlinear Materials
for Practical Quasi-Phase-Matched Mid-IR Devices

ONR Grant N00014-94-1-0426
Final Technical Report

Personnel Associated with the Program

Robert L. Byer	Principal Investigator, Professor of Applied Physics
Robert S. Feigelson	Professor (Research) of Materials Science and Engineering
Robert C. Eckardt	Senior Research Associate Ginzton Laboratory
Roger K. Route	Senior Research Associate Center for Materials Research
Lawrence E. Myers	Graduate Student (Ph. D. 1995) Electrical Engineering
Leslie A. Gordon	Graduate Student Applied Physics
Dong Zheng	Graduate Student Electrical Engineering
Sermon Wu	Graduate Student Applied Physics

Diffusion-Bonded Nonlinear Materials for Practical Quasi-Phase-Matched Mid-IR Devices

Robert L. Byer
Principal Investigator

I. Introduction

High-average-power coherent sources are needed throughout the infrared, especially in the 3 to 5-μm region, where atmospheric windows will permit remote sensing, and military countermeasures. Nonlinear frequency conversion of existing lasers can provide these sources. Optical parametric oscillators (OPO's) are attractive because they can provide output tunable over a wide range; however, currently available infrared (IR) nonlinear materials, e.g. the chalcopyrites $AgGaS_2$, $AgGaSe_2$, and $ZnGeP_2$, are limited by low surface damage thresholds, large absorption coefficients, or low thermal conductivity. GaAs and ZnSe have high thermal conductivities and low absorption coefficients, and are widely used for windows and mirrors in high power IR laser systems. These cubic crystals also have large second order nonlinear susceptibilities; however, they cannot be birefringently phasematched, and, therefore, have not been used in practical frequency conversion applications.

An alternative to birefringent phasematching is quasi-phasematching[1-3], where a periodic modulation of the nonlinear susceptibility compensates for the phase velocity mismatch between the interacting waves. Stacks of discrete plates at the Brewster angle have been used to quasi-phasematch second harmonic generation (SHG) in GaAs[4, 5]and CdTe[6], but reflection and scattering losses associated with the many interfaces in the air-spaced layers and the high indices of refraction, precluded wide-spread application in devices that would consist of 50 or more individual plates.

Four years ago we proposed diffusion bonding as a means to reduce loss, and fabricate a practical monolithic device. Extensive modeling calculations and initial diffusion-bonding and non-linear conversion demonstrations were funded under ARO DAAL03-92-G-0400. Results were encouraging; however, losses remained excessive. With ONR support through the research program summarized here, and through CNOM, the Center for Nonlinear Optical Materials at Stanford (N00014-92-J-1903), we have made

considerable progress in reducing optical losses in these structures, and we now believe continued development of high power diffusion-bonded-stacked (DBS) GaAs devices for quasi-phasematched (QPM) interactions is justified. Until additional funding can be developed, the research is being carried forward at a reduced level with ONR support through CNOM.

II. Background

QPM is achieved by a periodic modulation of the nonlinear susceptibility which compensates for the phase velocity mismatch between the interacting polarization waves, allowing efficient interactions in the absence of phase-velocity matching. Optimally, the modulation of the nonlinear susceptibility is a sign reversal, with a period L equal to twice the coherence length, L_c. The coherence length is the distance over which a π phase difference develops between the fundamental and the harmonic polarization waves, and is related to Δk, the wave vector mismatch due to material dispersion, by

$$L_c = \pi/\Delta k, \qquad \text{where} \qquad \Delta k = k_1 - k_2 - k_3 = (n_1\omega_1 - n_2\omega_2 - n_3\omega_3)/c,$$

where n is the refractive index, k is the wave vector, c is the speed of light in vacuum, and subscripts refer to quantities evaluated at the three interacting frequencies; we use the convention $w_1 > w_2 \geq w_3$. For efficient QPM, one of the spatial harmonics $K_m = 2\pi m/L$ of the periodically modulated medium must lie close to Δk, where m is an integer and is the order of the quasi-phasedmatched interaction. If this condition holds, quasi-phasematched nonlinear interactions behave similarly to conventionally phasematched nonlinear interactions, but with an effective wave vector mismatch $\Delta k_Q = \Delta k - K_m$, and an effective nonlinear susceptibility d_m equal to the amplitude of the mth Fourier component of the nonlinear susceptibility. For odd-order QPM (m = 1, 3,...) with 50% duty cycle, $d_m = 2d_{eff\text{-}b}/m\pi$, where $d_{eff\text{-}b}$ is the effective nonlinear coefficient for the homogeneous bulk material. Detailed analyses of QPM appear in Refs.[2, 3].

The dispersion properties of some potential diffusion-bonded stacked (DBS) materials are shown in Fig. 1. These curves were generated using dispersion equations given by Pikhtin and Yas'kov[7]. The regions of low dispersion near the center of the curves indicate the useful spectral region for that material. The flatter the dispersion curve, the longer the coherence length, and the fewer bonds necessary for a given length of crystal. The coherence lengths determine the feasibility of the DBS structure. The longer the L_c, the easier the wafer is to polish and handle, and the more tolerent the final device is to absolute thickness errors.

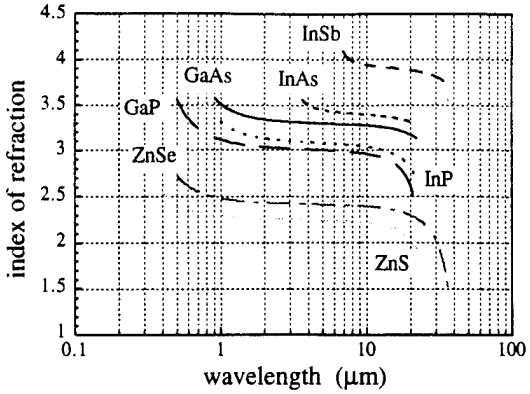

Fig. 1. Dispersion curves for III-V and II-VI semiconductors.

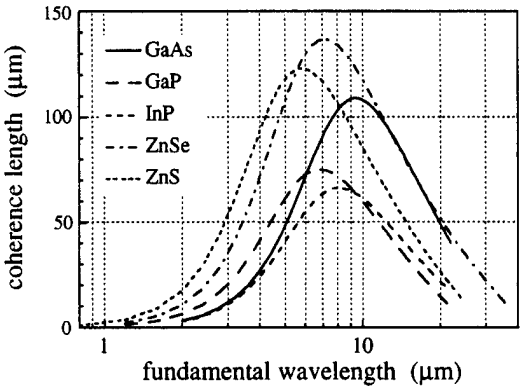

Fig. 2. Coherence lengths for second harmonic generation of the mid IR in GaAs, GaP, InP, ZnSe, and ZnS.

Second harmonic generation evaluates the nonlinear properties of new material, while avoiding problems of thresholds and loss which are critical for parametric generation. Coherence lengths for SHG, calculated from the dispersion relationships, are shown as a function of fundamental wavelength in Fig. 2. GaAs, ZnSe, and ZnS are attractive because of their long coherence lengths. Both ZnSe and GaAs have high damage thresholds at 10.6 and 5.3 μm; however, single crystal ZnSe is not yet readily available. The coherence length for SHG of 10.6 μm in GaAs is 106 μm and since two-side polished GaAs wafers 300μm to 600 μm thick (third and fifth order QPM) are commercially available, the experimental component of the program was focused on that material.

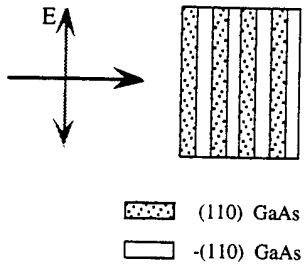

Fig. 3. Basic DBS structure in GaAs showing the layers of alternating nonlinear coefficients.

Figure 3 shows a schematic of the basic DBS nonlinear structure. GaAs has $\bar{4}3m$ symmetry which means that the maximum nonlinear coefficient occurs for radiation polarized along a <111> direction. {110} wafers were chosen for the nonlinear studies because they provide the maximum effective nonlinear coefficient for propagation normal to the input face. Adjacent wafers were rotated by 180° to alternate the sign of the effective nonlinear coefficient.

Our early ARO-supported studies developed a diffusion bonding process similar to some two-wafer bonding techniques employed in the optoelectronic device industry [8-10]. DBS structures containing between 2 through 9 layers were bonded into monolithic units. Although the thickness of the layers was not optimal, we measured the relative SHG power for 2 through 9 layer DBS GaAs[11]. The agreement with the expected dependence on the number of layers demonstrated that DBS GaAs acts as a monolithic structure with a modulated nonlinear coefficient, providing phase coherent interaction. While we had verified that the nonlinear coefficient, and therefore the crystal lattice was unaffected by the bonding process, bonding was not always uniform; significant scattering was still present due to gaps and voids at the interfaces, and transmission losses were greater than 5% per layer.

III. Diffusion Bonding Development

Most of the process development and materials testing was carried out by bonding small stacks of two or three wafers. A variety of undoped and lightly doped GaAs wafers were used. They were all mechanical or epi-grade and polished on both sides. We were able to bond wafers regardless of their doping, alignment of the crystalline axes, and orientation: {100} to {100}, {110} to {110} and {110} to {100}. The quality of the bonded interfaces was evaluated by examining various physical properties: a) mechanical strength as evidenced by resistance to fracture under thermal shock and mechanical stress; b) absorption, scattering and wavefront distortion as observed interferometrically to measure optical quality; and c) microscopic uniformity as determined by examination of cleaved cross-sections using optical microscopy, scanning surface electron microscopy (SEM) and transmission electron microscopy (TEM). Most of our early bonds appeared adequate with respect to mechanical strength, and low-power planar transmission microscopic examination. We found numerous medium-to-small voids (2 - 0.2 μm diameter), and thin gaps (approx. 0.2 μm) between the surfaces when we observed cleaved cross-sections under higher power microscopy or SEM. With the process improvements accomplished during the last program year (1995), significant improvements in uniformity and reductions in the defect density at the bonded interfaces were accomplished. We still find small voids (generally ~0.2 μm in diameter) in varying densities, but improved pressure uniformity has virtually eliminated the ~0.2 μm gaps at the interfaces.

There are three stages to the diffusion bonding process developed during this program: preparation of the wafers, assembly of contacted stack, and high temperature annealing. During the last program year, significant improvements to the bonding process were made in all three areas. Commercial, epi-ready two-side polished gallium arsenide wafers were diced into 1-cm^2 pieces using a diamond wafering saw. Thorough cleaning and degreasing were found to be critical to achieve well-bonded interfaces. A four-step cleaning sequence similar to that used in semiconductor processing was found to be effective:

1) soap and de-ionized water
2) trichloroethane
3) acetone
4) methanol or propanol.

Prior to contacting, the diced wafers were etched to remove surface oxides using dilute concentrations of HF, HCl, or NH_3OH. After the wafers were etched, they remained fully immersed in a solvent while they were assembled in the bonding fixture.

The stack was then pressed together to expel the excess liquid before being removed from the solution. Suitable solvents were: de-ionized water, methanol and propanol. Uninterrupted immersion minimized the chances of any particulates adhering to the surfaces, and slowed the regrowth of native surface oxides.

During the annealing process the wafer surfaces are held together under pressure and elevated temperatures. There are three stages to the bonding process. Dipole-induced dipole or Van Der Waals bonds form when the surfaces are first brought together. This is commonly called optical contacting, and can be broken by rapid temperature cycling. As the wafers are heated under pressure, the bonding electrons will move between, and become shared between the two surfaces forming a chemical bond. These individual bonds are as strong as any bond in the GaAs crystal; however, no mass transport has occurred and therefore, no filling-in of void spaces has occurred. Any surfaces that were not atomically flat, will still have voids at their interfaces. During the final stage, there is a re-arrangement of the atoms by mass transport to fill the interfacial voids. This stage occurs more rapidly above the congruent evaporation point (640°C for GaAs, where As evaporating off the surface may permit the remaining Ga to rapidly diffuse to new positions). If the bonding is performed under an As overpressure, less As evaporates, and mass transport is much slower [12].

Interfacial Gaps and Voids

To obtain perfect interfaces, it is necessary to eliminate all the gaps and voids created when surfaces which are not atomically flat are brought together. Voids can also trap gases and solvent residues between the wafers. Systematic modifications in the wafer bonding procedures were investigated to minimize the formation of these defects and the resultant optical scattering losses. Processing variations have been used previously to study interfacial defects found in the grain boundaries of polycrystalline ceramics[13-16]. These defects were eliminated by heat-treatment (mass transport) processes according to classical sintering theory[13]. Table I lists the alternate paths for mass transport during any sintering process. The dominant path(s) depends on the relative transport rates which are a strong function of temperature, time, vapor pressure of the materials involved, and total system pressure. To elucidate the sintering mechanisms in alumina, Rodel, Glaeser, and Powers[14-16] introduced interface voids of various shapes by bonding topographically patterned sapphire wafers to flat sapphire surfaces at elevated temperature. They found that mass was transferred from flat surfaces to fill in nearby corners which had the effect of "rounding out" the voids. The mass redistribution reduced both the cross-sectional area of the voids as well as their volume.

Table I. Alternate paths for mass transport during the sintering process.[13]

Mechanism Number	Transport Path	Source of Matter	Sink of Matter
1	Surface diffusion	Surface	Neck
2	Lattice diffusion	Surface	Neck
3	Vapor transport	Surface	Neck
4	Boundary diffusion	Grain boundary	Neck
5	Lattice diffusion	Grain boundary	Neck
6	Lattice diffusion	Dislocations	Neck

During the program described here, a similar approach (using a series of controlled interfacial voids) was used to investigate interfacial defect behavior during the wafer-bonding process. Artificial voids were introduced by bonding topographically patterned GaAs wafers to unpatterned wafers as shown in Fig. 4. In preliminary work, we measured the changes in the size, shape and structure of the voids as a function of the wafer-bonding process variables. It was found that the relative fraction of well-bonded areas, (total well-bonded area in void)/(original void area), in 800-Å deep voids began to increase only when process temperatures exceeded 910 °C. We found that increasing the processing temperature above 910 °C and/or increasing the processing time improved the relative fraction of well-bonded areas.

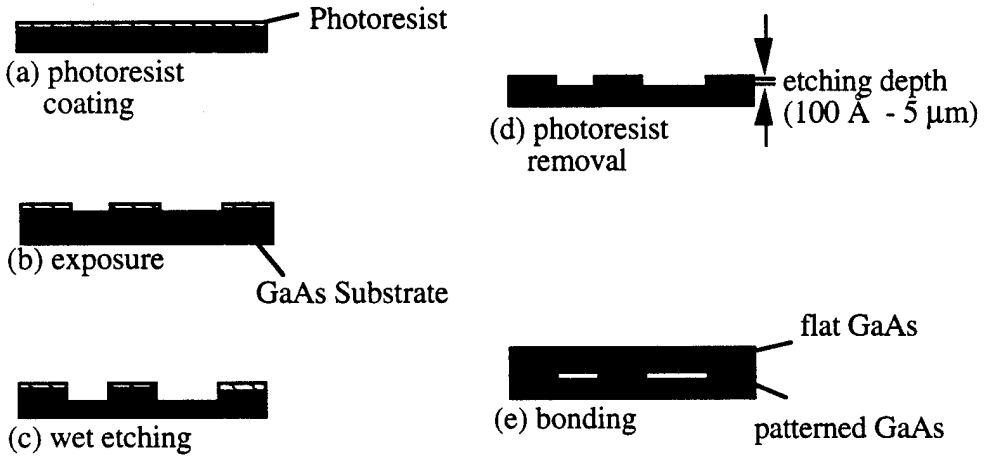

Fig. 4. Illustration of the steps in fabrication of artificial interfacial defects (i.e. voids).

Following initial experiments, we carried out a more in-depth look at the effects of processing parameters on microstructure and optical quality. The processing parameters that were varied included bonding temperatures between 630-975°C, pressures of 0-25 Kg and time. Our earlier study of artificial voids was extended to include a range of depths between 100-1000Å. Changes in the artificial voids were characterized by transmission optical microscopy (TOM) and high resolution transmission electron microscopy (HRTEM).

We found that the relative fraction of well-bonded areas increased slowly with time, consistent with the relatively low diffusion coefficients of GaAs [17-19]. As mentioned previously, we found that the relative fraction of well-bonded areas in 800-Å-deep voids did not start to increase until process temperatures reached 910 °C. Figure 5 shows transmission optical micrographs of wafers with 700-Å-deep artificial voids bonded at 870 °C and 910 °C, respectively. The dark regions seen in the photographs are unbonded areas, while the light regions are well-bonded. The relative fraction of well-bonded areas clearly increased with temperature, consistent with the fact that the diffusion constants increase with temperature[17-19]. The relative fraction of well-bonded areas in shallower 100-Å-deep voids began to increase at 850 °C, and it increased as a function of time as well, as shown in Figure 6.

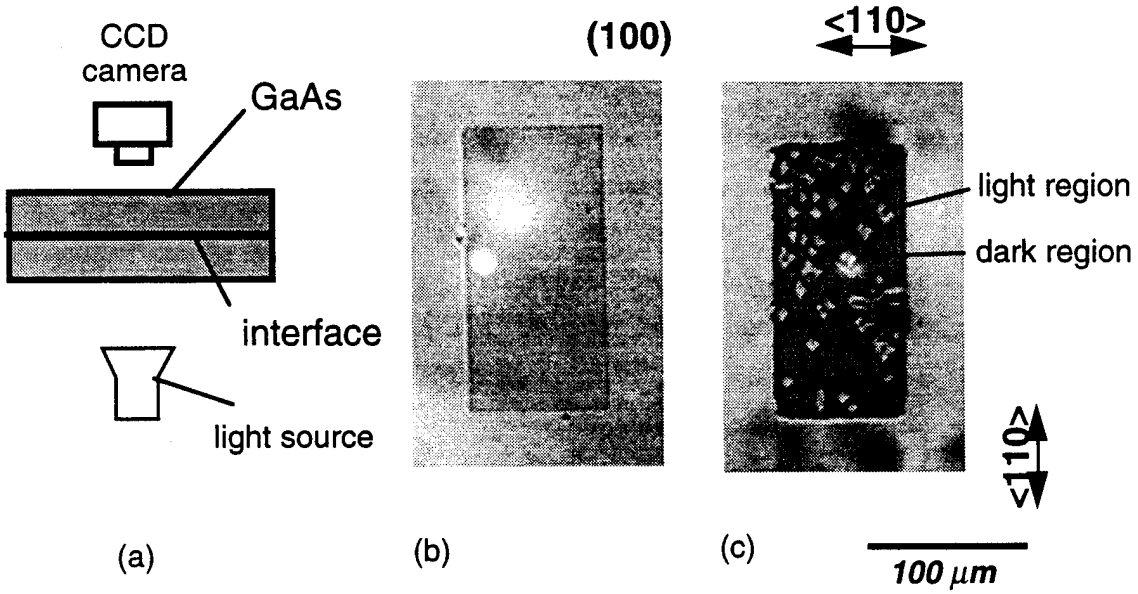

Fig. 5. (a) Transmission optical microscope set-up and images of the interfacial voids (700 Å deep) after bonding at various temperature:(b) 870 °C and (c) 910 °C.

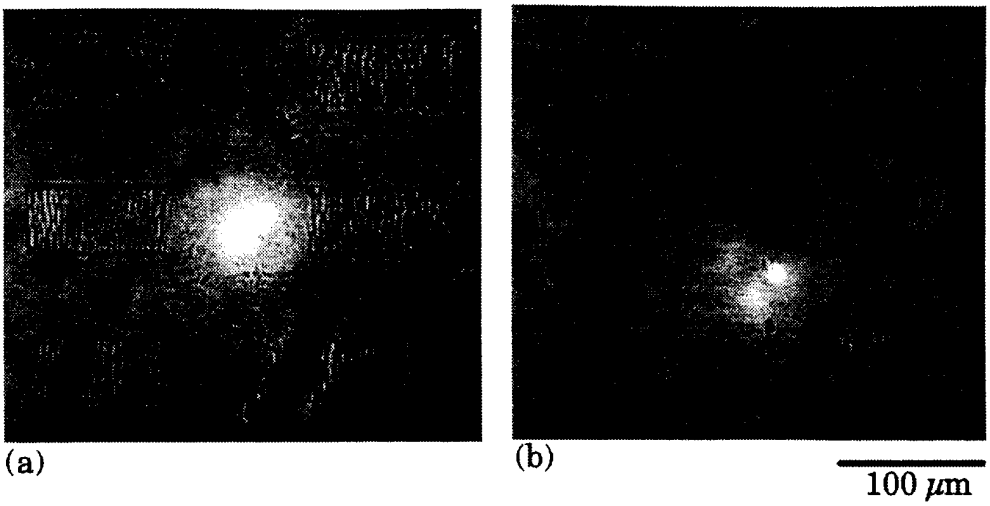

Fig. 6. Infrared transmission optical micrograph of artificial voids (100 Å depth) in GaAs wafers bonded at 850°C for various times: (a) 2.5 hour and (b) 7.5 hour.

Figure 7 is an HRTEM of a cross-section of the light region, or well-bonded part of the interface. On an atomic level the interface is very clean. Disordering exists for only a few atomic layers on either side of the interface.

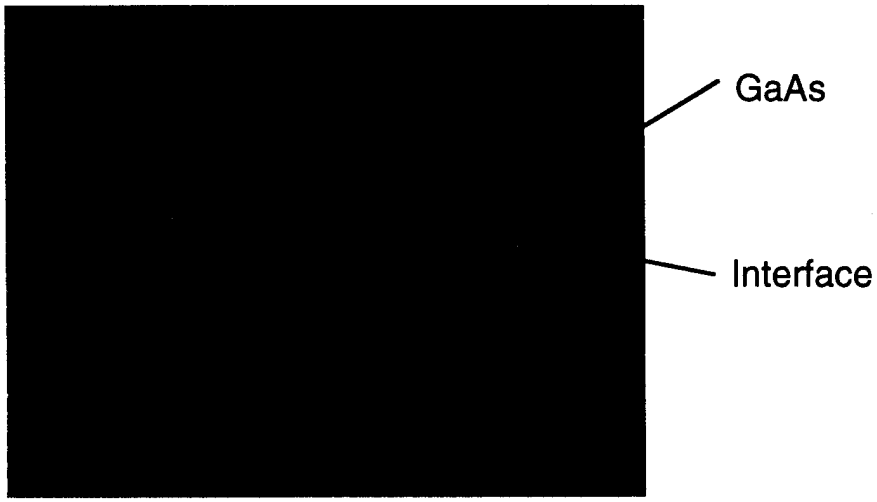

Fig. 7. Cross-sectional high resolution TEM of bonded wafers in light regions

Annealing Parameters

During the annealing stage the interface and bulk device quality can be affected by a number of parameters. We have investigated variations in environment, bonding pressure, temperature and time. Below is a synopsis of our results.

1) environment

a) physical composition of the sample holder and anvils (spacers):

- Bulk loss seem to be affected by the material in contact with the GaAs wafers during annealing.
- Bulk loss may be affected by the porosity of the material in contact with the GaAs during annealing.

b) composition of atmosphere:

- No measurable distinction was found in the range of 0 to 20% H_2 in N_2.
- No differences were observed using Ar instead of N_2.
- There may be some benefit in processing in As or Ga atmospheres, however, there are indications of these atmospheres inhibiting the bonding process[12].

c) atmosphere flow rate:

- The bonding furnaces are typically operated in a slight over-pressure, purge mode. If purge rate is insufficient, oxygen can back-diffuse into the furnace forming an amorphous oxide coating on the sample.
- If flow is too high, volatilized arsenic is swept away leaving an eroded Ga-rich outer surface.

2) uniaxial bonding pressure

a) magnitude:

- Successful bonding has been observed at pressures from 0.2 to over 50 kg/cm^2.
- A minimum pressure is necessary to maintain contact during processing, probably dependent on surface preparation and flatness, and processing temperature.

b) uniformity/distribution:

- Improved macroscopic pressure uniformity correlates with improved physical and optical uniformity of the bonds.
- A technique has not been developed to assess the microscopic pressure uniformity and its influence on optical properties.

3) temperature

a) magnitude:

- High quality bonds have been formed at processing temperatures between 700 to 975°C.
- Interfacial defect size and density diminish as processing temperature increases; however, optical loss due to bulk absorption increases.

b) uniformity/distribution:

- Temperature uniformity in our bonding furnaces is $<\pm 5°C$ across the sample at 850°C.
- The use of high transverse temperature gradients was avoided in this study. However, it is possible that microscopic interfacial voids could be eliminated by a temperature gradient transport technique.

4) time

a) variable bonding pressures:

- Uniaxial bonding pressures, controlled as a function of temperature and time, were employed during the annealing cycle to avoid exceeding the relatively low fracture strength of GaAs in its brittle, low temperature (<650°C) regime.
- An appropriate pressure/time/temperature cycle may minimize frozen-in mechanical stress.

b) heating and cooling rates

- Heating and cooling rates affect residual stresses in semiconductor crystals, which will affect the bulk optical properties of diffusion bonded stacks. Slow heating/cooling rates (<200°C/hr) were used for the multi-layer stacks.
- Quenching from elevated temperatures may offer a possible mechanism to freeze-in defect equilibrium distributions existing only at elevated temperatures.

c) soak time:

- Maximum bonding temperatures have been maintained for periods of 0.5 to 19 hours.
- Beyond a minimum time which is dependent on temperature, the properties at the bonded interfaces do not change significantly.

IV. Furnace Design and Development

With increased understanding of the bonding process, improved repeatability and optical quality were more easily obtained. Modifications of the furnace design have been necessary to implement techniques required for improved bonding. Three iterations in furnace design have been developed, evaluated, and employed during this program.

The original furnace, illustrated in Fig. 8, was constructed using a four inch diameter quartz tube surrounded by a resistive heating element. Optically bonded samples are supported by anvils of graphite, alumina, or sapphire in holders fabricated from boron nitride or graphite. Weights are placed on top of the holder, and the assembly is slid into the oven on a graphite slab. Gas flow rate is 1 l/min. This oven provided stable, repeatable temperatures and a low gas flow rate adjacent to the samples. However, bonding pressure could not be applied uniformly, and it was not adjustable during the annealing procedure.

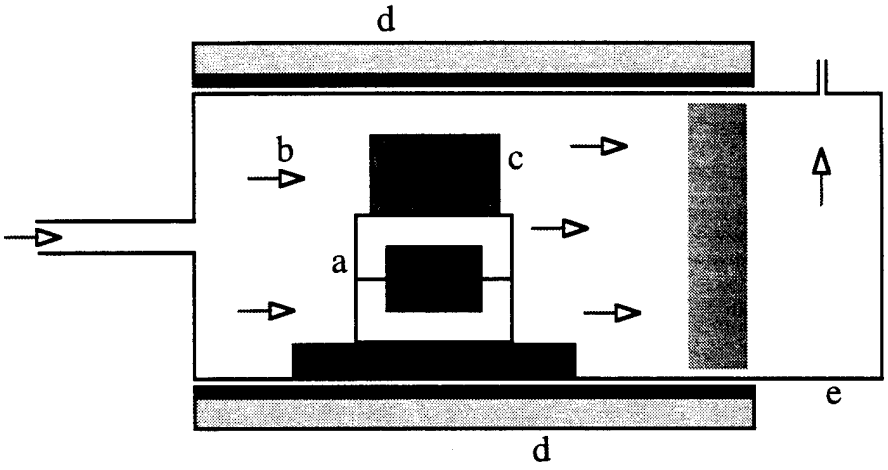

Fig. 8. Original furnace used for bonding. (a) Sample holder, (b) Gas flow, (c) Weight, (d) Heating element and thermal insulation, and (e) Quartz tube.

The second generation furnace illustrated in Fig. 9 addressed the problems encountered with the original furnace. The sample pressure was more uniform and was infinitely adjustable during the bonding process. It was lamp-heated to permit very rapid thermal cycling. Additionally, the tube was sealed and could be operated from 10^{-3} torr to atmosphere.

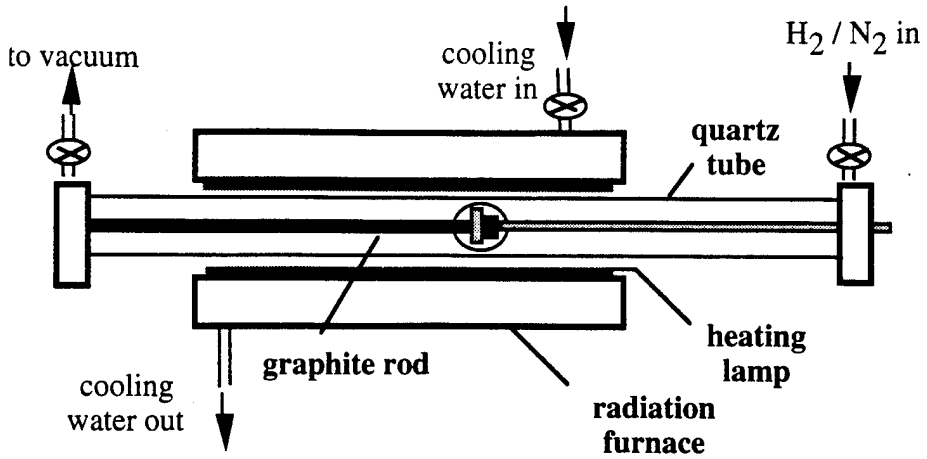

(a) radiation furnace

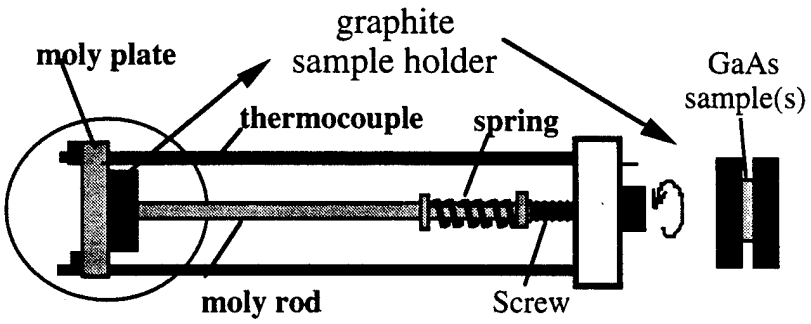

(b) sample holder

Fig. 9. Second generation wafer-bonding furnace. (a) This furnace provides rapid thermal cycling, and atmospheric pressure control, including vacuum. The sample holder (b) is inserted into the quartz tube. Pressure on the GaAs sample is adjustable to 10 kg/cm^2 by the screw at the end of the sample holder.

Typical wafer bonding processes included the following steps:

1. Initial vacuum degassing at room temperature,
2. Surface reduction by slowly heating up to 600°C in a pure H_2 atmosphere under reduced pressure (0.06 atm.),
3. Bonding under flowing H_2(60 cc/min.)/N_2(1l/min.) at atmospheric pressure and elevated temperature, and
4. Post-processing cool-down at the rate of ~10°C/min..

Details of the wafer-bonding process (temperature, compressive load, time, atmosphere, and heating/cooling rate) are illustrated in Fig. 10.

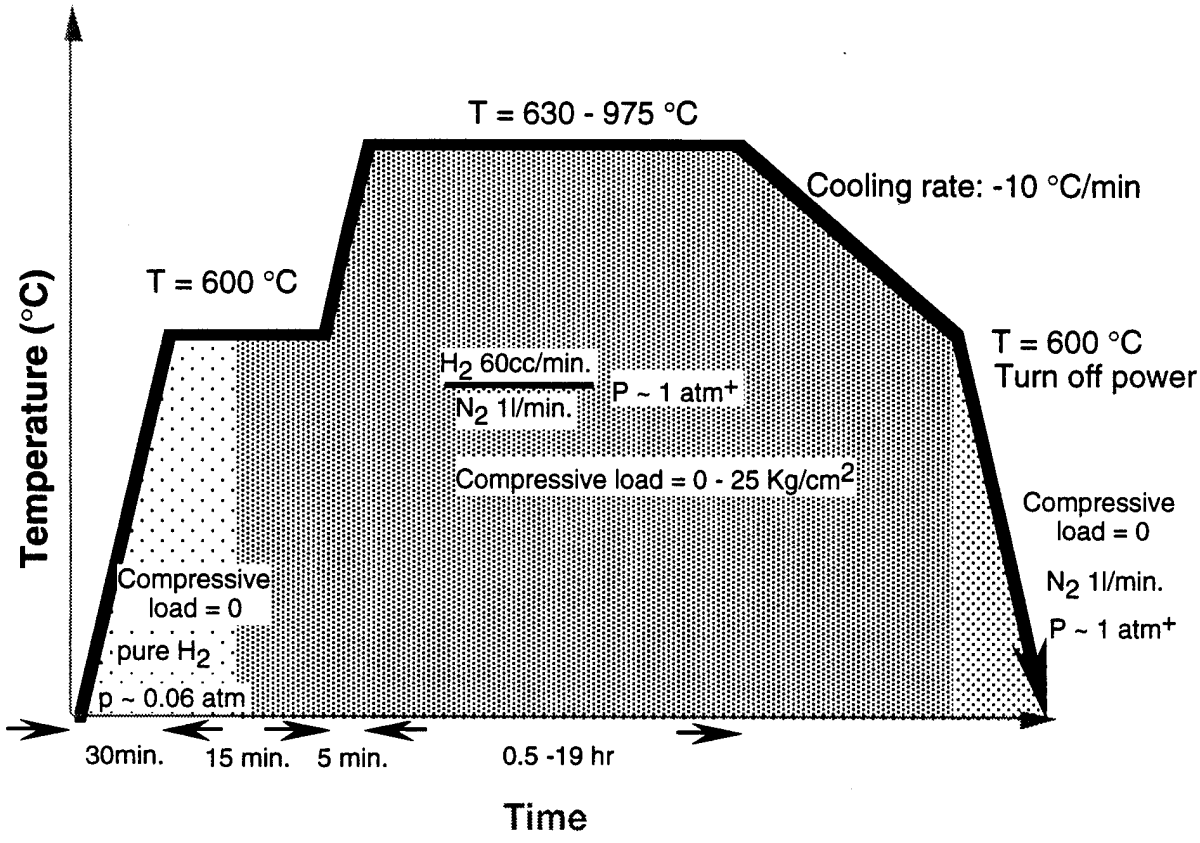

Fig. 10. Typical bonding cycle used with the second generation furnace.

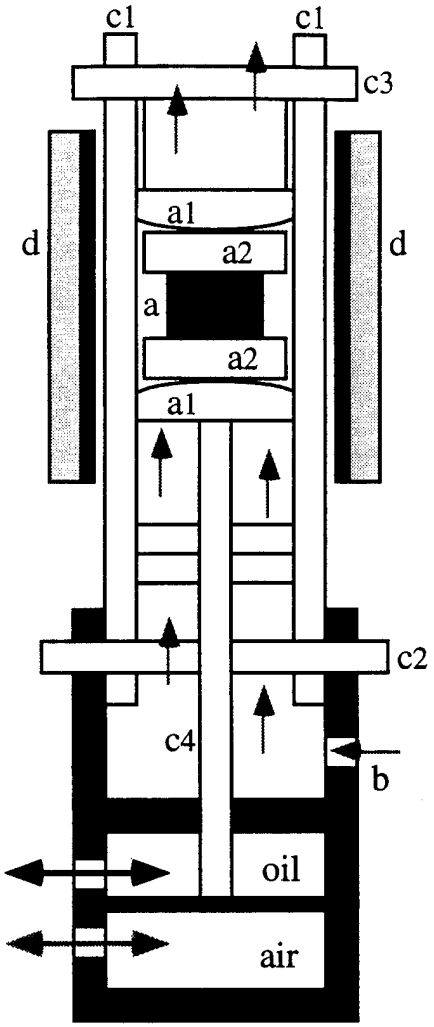

Fig. 11. The third furnace used for diffusion bonding.

A third generation furnace (Fig. 11) was designed and built to provide very uniform pressures up to 10^7 N/m^2 (100 kg/cm^2). Quartz was used extensively in the construction of this furnace. The 32-mm-outside-diameter, 5-mm-wall tube (c1) is both the oven wall and the main structural member. The outer push pieces (a1) are flat on the outer side and slightly convex on the inner side. The inner push pieces (a2), which contact the sample or the spacers (a), are slightly smaller than the outer ones and are therefore free to tilt on the convex surfaces permitting a macroscopically uniform pressure to be applied to the sample. Pressure is transfered from the pneumatic piston (c) through the push rod (c4) to the push pieces. The tube (c1) is attached to the piston (c) by means of an aluminum ring and pins (c2). The upper outer push piece is held in position by a spacer that is restrained by the top pin (c3). This furnace has very low thermal mass for rapid temperature cycling. The pressure is applied from the outside, and can be adjusted at any point during the process. The furnace can maintain sample temperatures of up to 1000° C.

We have been able to produce samples with much more uniform bonds with both the second and third generation furnaces. However, we still observe very small (< 0.2 μm) voids uniformly distributed along the interface. The interface quality is much improved and very repeatable compared with that obtained from the original furnace design. Due to the furnace/holder design, however, the sample in the third generation furnace is exposed to higher gas flow rates than in the earlier two furnaces, and this leads to higher rates of arsenic loss and surface erosion. We are currently modifying the furnace seals to permit operation with no gas flow, or with the chamber under vacuum.

Table II. Comparison of furnaces used in diffusion bonding studies

Furnace model	1	2	3
Pressure application	weights	spring	pneumatic piston
Pressure range ($N/m^2 = Pa$)	$0 - 10^5$	$0 - 3 \times 10^6$	$0 - 10^7$
(kg/cm^2)	0 - 1	0 - 30	1 - 100
Pressure uniformity	not uniform	better uniformity	very uniform
Approximate gas speed at sample surface (mm/min)	> 0.12	> 0.49	2.3
Heater type	resistive wire	lamps	resistive wire
Maximum heating rates (minutes: 25 to 840°C)	20	10	< 15
Maximum cooling rates (minutes: 840 to 25°C)	180	10	30
Maximum temperature (°C)	>1000	1000	1100
Orientation	horizontal	horizontal	vertical / horizontal
Vacuum capability	no	yes	yes

V. Optical Transmission Loss

Low absorption and scattering losses are critically important for quasi-phasematched nonlinear-optical applications of diffusion bonded stacked (DBS) semiconductor materials. Practical nonlinear devices will require stacks of 50 to 100 layers or more. An important component of this program was an investigation of the origin of scattering and absorption losses that result from the wafer bonding process. Figure 12 illustrates two kinds of defects that were found to affect optical losses in bonded stacks of GaAs wafers: (1) bulk defects within individual wafers, and (2) interfacial defects between individual wafer surfaces. Bulk defects may include dislocations, vacancies, interstitials, anti-sites, precipitates, and impurities. Dislocations can be generated during wafer bonding by plastic deformation[20-22], while vacancies, anti-sites, interstitials and precipitates can be caused by incongruent evaporation of Ga and As from exposed surfaces. At typical processing temperatures, the evaporation rate of arsenic is higher than that of gallium[23, 24]. Impurities may originate from within the GaAs boule itself, or they may diffuse in from the wafer surfaces. Interfacial defects consist of gaps, voids and inclusions. They can be caused by incomplete bonding, surface irregularities, surface

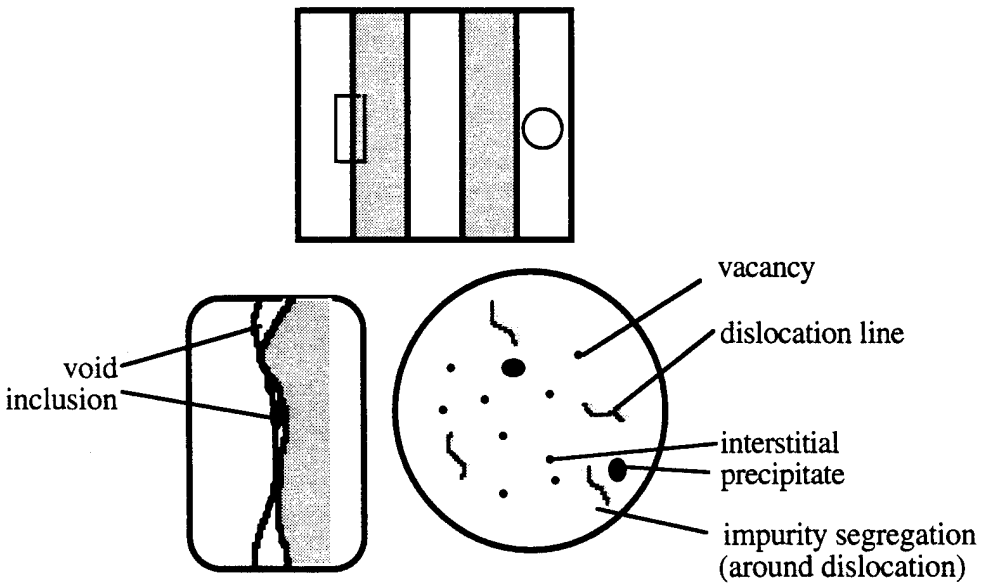

Fig. 12. Schematic illustration of two kinds of defects that contribute to optical losses : (a) interfacial defects between the bonded wafers, and (b) bulk defects within the wafers

contamination, surface oxides, or gases and solvent residues trapped between the wafers.

A 20-layer GaAs diffusion bonded stack composed of alternating 300-μm and 340-μm thick Atomet (110)-oriented plates was fabricated at 835° C for optical evaluation. The total stack thickness was 6.4mm and its average period was 320 μm which is close to the 318 μm coherence length for SHG of the CO_2 laser. Its transmission spectrum is shown in Fig. 13.

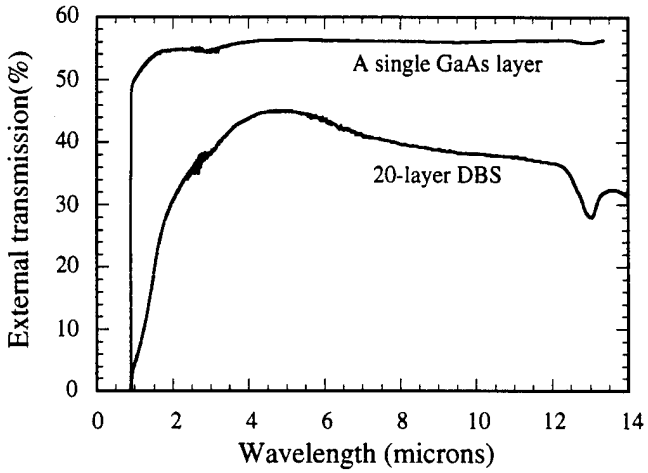

Fig. 13. Transmission spectra of a 20-layer diffusion bonded stack of (110) GaAs wafers and a single layer GaAs wafer

It is useful to compare the absorption measurements of Fig. 13 with calculations of scattering losses. This comparison is facilitated by the log-log presentation of the data in Fig. 14. At wavelengths shorter than 2μm, its transmission spectrum approximates the expected loss due to Rayleigh scattering. Rayleigh-type scattering can originate from voids at the interfaces, which were observed on cleaved cross-sections of single interfaces using optical microscopy. Average diameters were in the range of 0.5μm. In the 2μm to 3μm waveband, the transmission losses approximate expected losses due to gaps at the interface. Modeling suggests these losses can be due to one 180-nm wide gap, or nineteen 35-nm wide gaps. Most probably, they were caused by a range of gaps with different thicknesses. Given our current wafer preparation procedure, it is quite plausible this type of scattering defect exists since gaps having a variety of dimensions are readily observed in our single bond experiments. The overall transmission curve covering the 1-4 μm waveband is thought to be a combination of these effects.

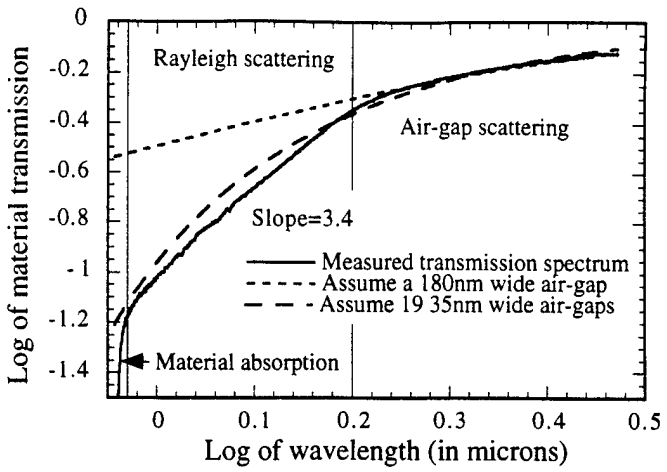

Fig. 14. Comparison of measured transmission losses in the 20-layer DBS GaAs sample with calculated Rayleigh scattering from small sperical voids and from loss due to thin gaps at the interfaces.

Analysis using single GaAs wafers

The reduction of transmission at wavelengths longer than 4 μm cannot be explained by voids or air gaps at the bonding interfaces. Interfacial scattering is wavelength dependent, and will decrease as the wavelength increases. This loss is process induced, and can be reproduced in single wafers. It is not a surface effect; wafers have been polished or etched to remove more than 50 μm of their outer surfaces with no significant improvement in their transmission. GaAs wafers from different sources exhibited different post-annealing transmission values; however, the effect was consistent within a given set of wafers fabricated from a single boule. In Fig. 15, we show the transmission of wafers from two different boules from the same supplier of nominally indentical undoped, semi-insulating GaAs. They were annealed for the same time, and in the same holder, to insure identical heat treatment at 834°C. The two sets of wafers had the same transmission spectra before annealing. One might conclude form the figure that sample orientation has an effect. However, many (110) and (100) wafers from different suppliers were investigated, and no orientation dependence was observed.

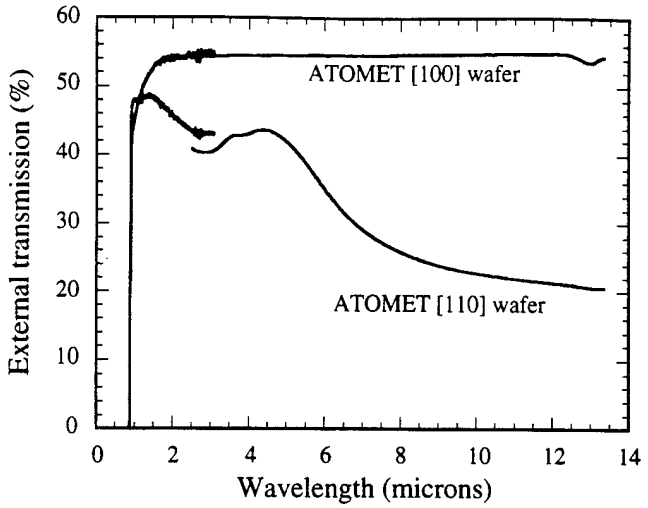

Fig. 15. Transmission spectra of different wafers after annealing at 834°C

The transmission of both GaAs wafer sets was next investigated as a function of annealing temperature. The temperature for the (110) wafers was varied from 700 to 834°C, Fig. 16, while the processing temperature for the (100) batch was varied from 850 to 975°C, Fig. 17. In both cases, this was the range of temperature required to reduce the process induced loss from overwhelming to barely detectable. In both cases the optical loss increased as a function of temperature. This was first attributed to an increase in the evaporation rate of Ga and As from the wafer surfaces with temperature. The evaporation ratio of As/Ga begins to increase significantly from unity when the temperature exceeds 640 °C[23, 24]. Incongruent surface evaporation results in roughened Ga-rich surfaces, potentially augmenting vacancies, interstitials, and precipitates in the bulk material[23, 24]. Additionally, the density of impurities diffusing in from the GaAs wafer surface increases with temperature. When GaAs is placed under a compressive load, plastic deformation increases with processing temperature[20-22], so that a greater density of bulk defects such as dislocations are likely to be generated and impurities are more likely to segregate around the dislocation lines. All of these defects were considered as possible sources for the degradation in optical transmission seen during heat-treatment processing.

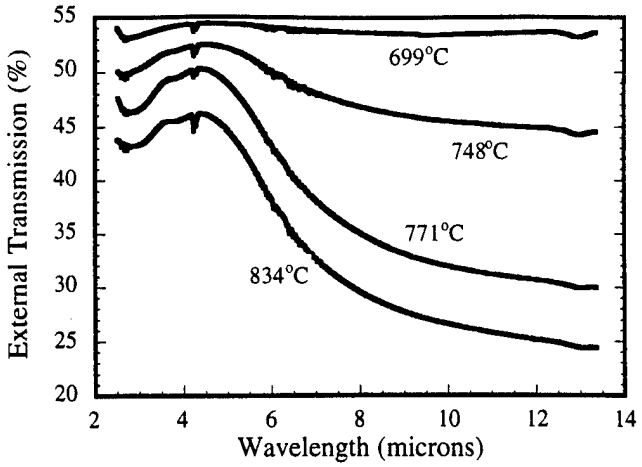

Fig. 16 FTIR transmission spectra for Atomet (110) single GaAs wafers processed from 700 °C to 834 °C.

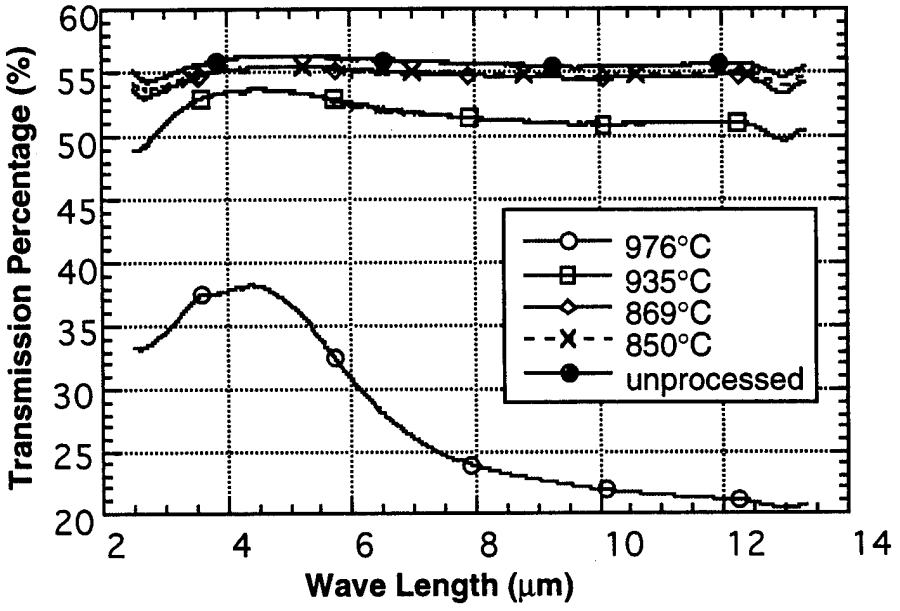

Fig. 17 FTIR transmission spectra for Atomet (100) single GaAs wafers processed from 850 °C to 975 °C.

Undoped semi-insulating GaAs typically has a carrier concentration of 10^{14}. When the Hall effect was used to determine the free electron and hole carrier concentrations, a surprising result was found. All of the wafers had become more p-type after annealing,

Table III. P-type GaAs is known to exhibit the signature longer wavelength absorption that we observed in our annealed samples. We therefore concluded that the losses observed in DBS GaAs at longer wavelengths are due to p-type free carrier absorption. Semi-insulating wafers convert to p-type during the annealing step, dependent on soak temperatures and durations, and quenching rates. Conversion is also affected by thermal history and composition of the wafers. During the manufacturing process GaAs undergoes various proprietary heat treatments to improve the uniformity, and the semi-insulating quality of the crystal. The p-type conversion is, therefore, supplier specific and varies from one wafer set to another. The semi-insulating to p-type transition has been well studied[25-27], and is reversible; however, the process for reversing the change depends on the thermal history.

Table III: Free carrier concentration measured by the Hall Effect voltage before and after annealing

Wafer Type	Processing Temperature (°C)	Conductivity Type	Sheet Conc.	Concentration (cm^{-3})
A: Atomet[110]	unproc.	n	3.00E+12	1.00E+14
B: Atomet[100]	unproc.	n	1.00E+12	1.00E+13
A: Atomet[110]	833	p	2.00E+15	5.00E+16
B: Atomet[100]	833	p	1.90E+13	2.10E+14
A: Atomet[110]	976	p	1.00E+15	3.00E+16
B: Atomet[100]	976	p	3.00E+13	1.00E+14
C: AXT[100]	833	p	9.00E+14	2.00E+16
D: Airtron[110]	833	n	2.00E+12	4.00E+13

To reduce the transmission losses due to p-type conversion we have considered a) generally reducing the annealing temperature to minimize the conversion, or b) establishing a post-bonding annealing treatment to regain the materials semi-insulating quality. To reduce the annealing temperature, it will first be necessary to ascertain that it is possible to bond at lower temperatures, and to verify that the transmission through a large number of layers remains high. To test the concept of annealing in an arsenic atmosphere, it will be necessary to build a hot-wall system, which is currently being considered.

Analysis using bonded GaAs stacks

The optical transmission of the single GaAs wafer from the Atomet (100)-oriented set used in the previous study, and heat treated at 850 °C, was almost the same as that of an unprocessed GaAs wafer (within 1%) as shown in Figs. 17. The relative fraction of well-bonded areas in 100-Å-deep voids patterned on 2-wafer-stack interface was reasonably high in this temperature range, as well. Therefore, a 2-layer (100)-oriented unpatterned optical stack was set up for bonding at 850 °C. The percentage transmission of this stack is shown in Fig. 18. Its optical transmission, in comparison with a single wafer processed under the same conditions, was only 0.5% less which is within experimental error. Based on this finding, we undertook to bond a low loss optical stack of 52 GaAs (100)-oriented wafers at the optimum bonding temperature, 850 °C. (100)-oriented wafer stacks do not permit QPM. The purpose of this experiment was simply to test the feasibity of fabricating a relatively large stack having low optical losses. The bonded sample is shown in Fig. 19, and its optical transmission spectra is shown in Fig. 20. This very promising experimental result represents the largest number of GaAs layers bonded to date.

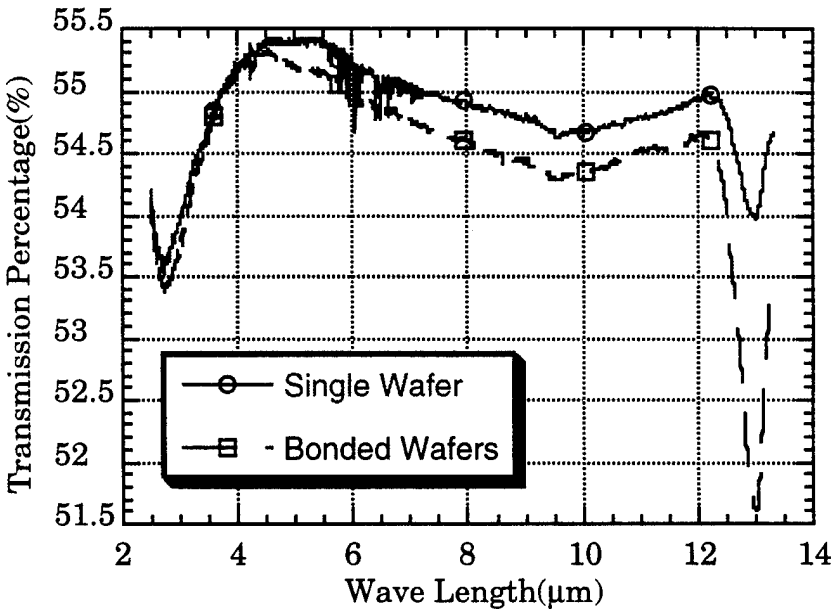

Fig. 18. FTIR transmission spectra for single wafer processed at 850 °C and two wafers bonded at 850 °C under a static 10 Kg load for two hours.

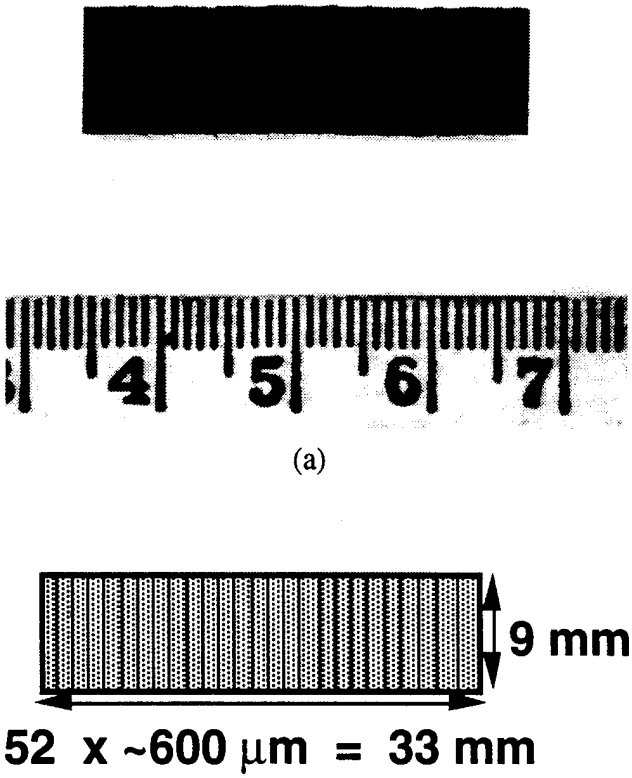

(a)

(b)

Fig. 19. (a)Photograph and (b) illustration of a 52 layer stack of (100) bonded GaAs wafers.

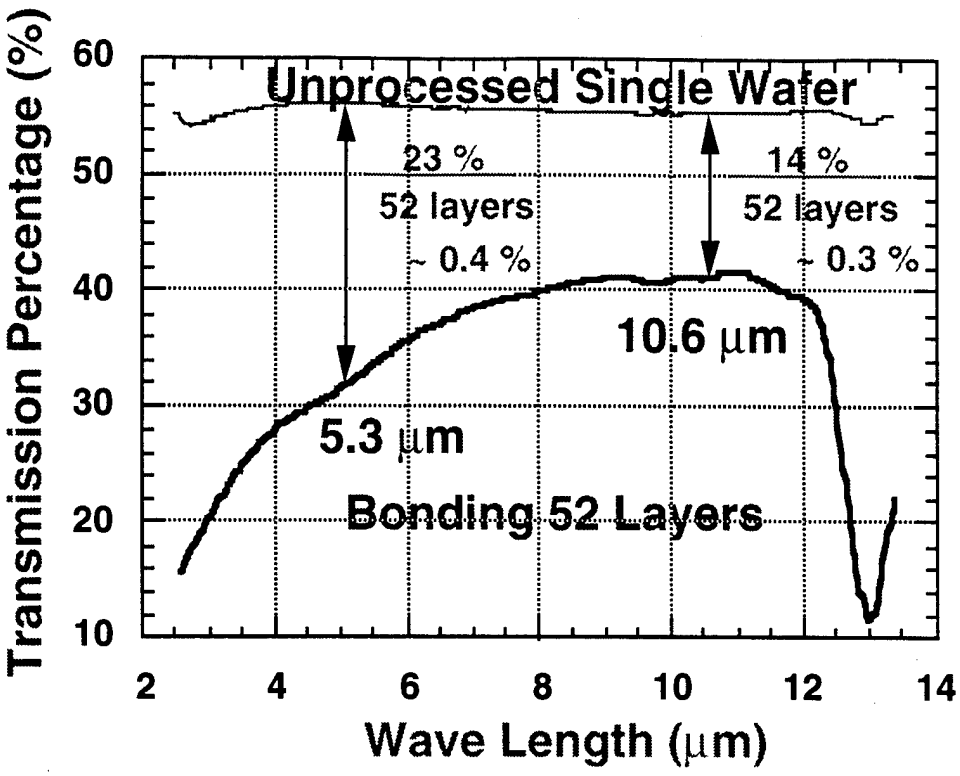

Fig. 20. Observed transmission of the (100)-oriented, 52-layer wafer-bonded GaAs stack shown in Fig. 19.

The studies on single Atomet (110)-oriented wafers indicated it would be possible to achieve a QPM stack with low losses in the mid-IR using this wafer set if we lowered the annealing temperature to the 700° C range to minimize the bulk absorption loss problem. Accordingly, we test-bonded a 15-layer stack at 700°C. The intent of this experiment was simply to evaluate optical losses, and therefore we used oversize wafers with average thickness around 340 μm since the wafer set contained a surplus of them. The transmission of this stack at wavelengths longer than 3 μm was found to be relatively flat, with a total internal loss of only 0.04 cm^{-1} at 5 μm, Fig. 21. This represents a loss of less than 0.2% per layer.

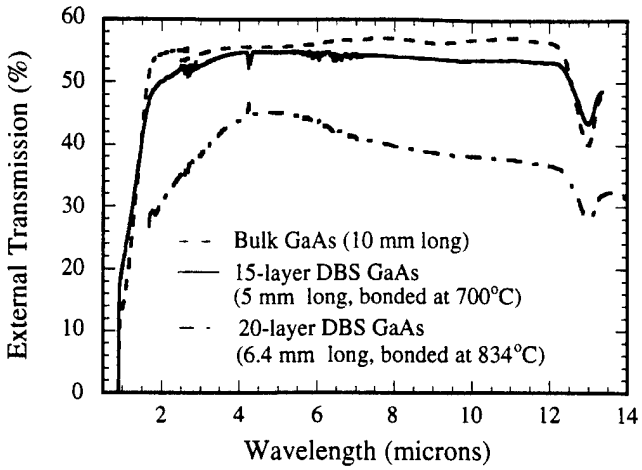

Fig. 21. Comparison of the transmission spectra of the (110)-oriented 15-layer DBS GaAs (bonded at 700°C), the (110)-oriented 20-layer DBS GaAs (bonded at 834°C), and a 1 cm long unprocessed bulk GaAs crystal

There remains some additional bulk loss at longer wavelengths which becomes apparent as we increase the thickness of the samples, indicating that p-type conversion has not been completely eliminated. Provided that we are able to bond these particular wafers at still lower temperatures, we could further improve the optical transmission. Future steps to improve the optical transmission will be a) to develop a post-bonding annealing process to re-establish the semi-insulating quality of the GaAs and b) most importantly to develop a better understanding of the individual manufacturers specific post-growth processing techniques that create the variation in the annealing behavior, which will in turn permit us to specify the optimal composition/thermal processing when ordering wafers from the vendors.

VI. Nonlinear Optical Device Testing

Second-harmonic generation of 10.6-μm CO_2 radiation was performed using the 20-layer stack that had the optimum average period but moderate mid-IR optical losses, to determine if the nonlinear properties of single crystal GaAs were preserved during the high temperature / pressure bonding process, and to verify the nonlinear conversion efficiency. The experimental setup is illustrated in Fig. 22. A 3-W CW waveguide CO_2 laser was chosen for its stable output. The 10.6-μm beam was loosely focused onto a 500-μm-diameter spot. The radiation propagation was incident normal to the sample. The DBS sample was rotated about a surface normal to observe the angular dependence of the second harmonic generation. Results of the angular scan are shown in Fig. 23. For comparison, Fig. 24 shows the 5.3-μm signal generated with a single GaAs plate of 320-μm thickness. It was later determined that four of the 20 layers had been incorrectly oriented. Therefore, the stack had effectively only 12 nonlinear layers, giving a predicted conversion efficiency 144 times greater than a single plate. The experimental results in Figs. 23 and 24 show the 20-layer stack had about a 120 times improvement in 5.3-μm harmonic generating efficiency over a single plate. An absolute power measurement showed the 20-layer stack generated 0.14 μW of 5.3-μm power, which is within experimental uncertainty of the theoretical prediction of 0.28 μW.

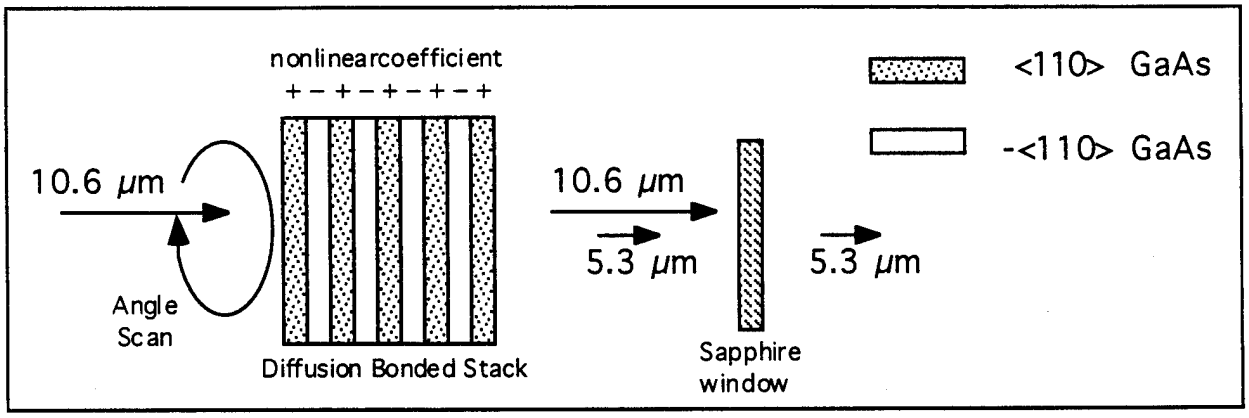

Fig. 22. Experiment set-up for doubling of 10.6μm radiation from a CO_2 laser

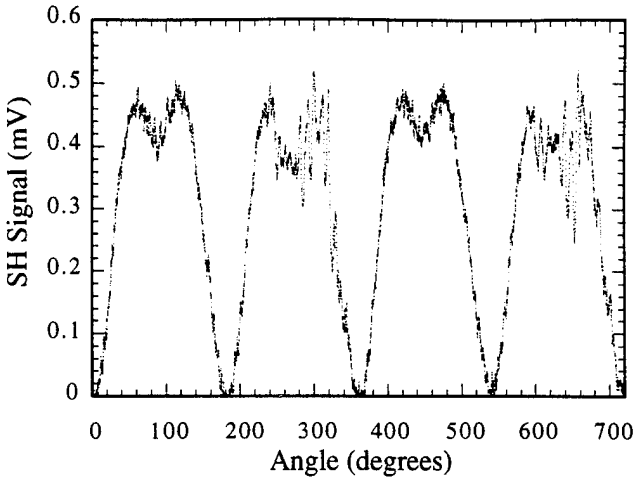

Fig. 23. 5.3μm second harmonic generation in a single layer of GaAs as a function of polarization angle. Effective input power is ~1W cw.

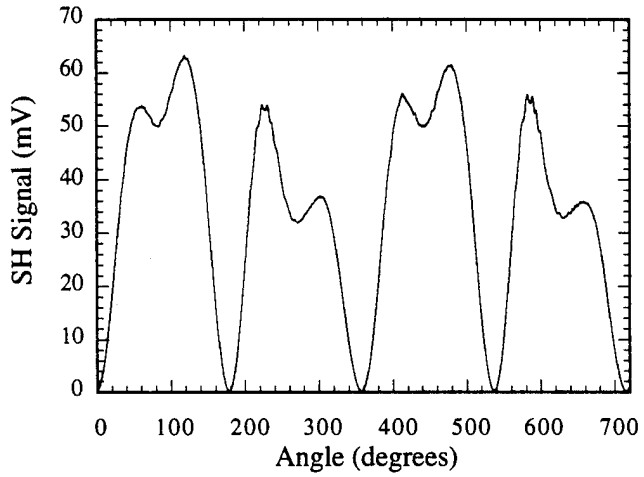

Fig. 24. 5.3μm second harmonic generation in a 20-layer DBS GaAs structure as a function of polarization angle. Effective input power is ~1W cw.

Similar studies on the 15 layer low-loss stack were deferred because of its limited length and non-optimum 340 μm period. A higher prioriity was attached to fabricating a larger, low-loss SHG stack with an optimum 318 μm period using the low temperature bonding process. However, this could not be completed within the program timeframe because we needed first to thin and repolish several wafers from the Atomet (110) set in order to generate a stack with the correct average period. These tasks will clearly receive high priority in our continuing ONR/CNOM-supported research.

VII. Conclusions and Recommendations for Further Study

In 1993, we proposed using diffusion-bonded-stacked GaAs for quasi-phasematched nonlinear optical conversion, to provide high peak and high average power sources in the the 3-5 μm region. Preliminary experiments demonstrated the feasibility of DBS structures in GaAs. Monolithic diffusion-bonded GaAs stacks with periodically alternating nonlinear coefficients retained both the thermomechanical and the crystalline properties of the bulk material, and provided phase coherent nonlinear interaction over ~0.4 cm. However, these early devices suffered optical losses of 2 to 5% per layer. Minimizing the optical losses became a major goal of this program.

Short wavelength loss was reduced by improving surface preparation. Techniques to dice, clean, etch and contact stacks of wafers were developed to minimize optical scattering at the bonded interfaces. For wavelengths greater than 3 μm, processing-induced p-type-free-carrier absorption was identified as the major loss mechanism. P-type conversion was reduced by lowering the bonding temperatures. Further improvements are expected with the implementation of a post-bonding annealing step, and with more detailed and optimized wafer specifications for the commercial suppliers.

Losses in our most recent diffusion bonded stacks have been reduced to less than 0.2% per layer at 5 μm, more than an order of magnitude improvement during the course of this program. At this level of loss, it is now possible to make practical DBS GaAs structures for pulsed nonlinear infrared applications. An additional order of magnitude reduction in optical loss will make high-average-power, cw nonlinear applications practical. It now seems feasible that we may ultimately approach the low levels of loss found in GaAs bulk crystals, something that has recently been achieved in quasi-phase-matched interactions in periodically poled lithium niobate. Continuing improvements in the processing of DBS structures are being pursued under interim ONR/CNOM funding.

Much of our bonding development work in GaAs can be applied to other semi-conductors. Modeling studies indicate that high conversion efficiencies can also be expected from ZnSe which has even higher damage thresholds than GaAs in the mid-IR, and longer coherence lengths, which eases the problems of wafer fabrication and handling for devices operating at wavelengths shorter than 5 μm. As single crystals of ZnSe become available from research laboratories in the US and Russia, an extension of these studies to the shorter wavelength regime using ZnSe is recommended.

VIII. References

1. J. A. Armstrong, N. Bloembergen, J. Ducuing and P. S. Pershan, Phys. Rev., 1962. 127(6): p. 1918-1939.

2. J. D. McMullen, J. Appl. Phys., 1975. 46(7): p. 3076-3081.

3. M. M. Fejer, G. A. Magel, D. H. Jundt and R. L. Byer, IEEE J. Quantum Electron., 1992. 28(11): p. 2631-2654.

4. A. Szilagyi, A. Hordvik and H. Schlossberg, J. Appl. Phys., 1976. 47(5): p. 2025-2032.

5. D. E. Thompson, J. D. McMullen and D. B. Anderson, Appl. Phys. Lett., 1976. 29(2): p. 113-115.

6. M. S. Piltch, C. D. Cantrell and R. C. Sze, J. Appl. Phys., 1976. 47: p. 3514-3517.

7. A. N. Pithkin and A. D. Yas'kov, Sov. Phys. Semicond., 1978. 12(6): p. 622-626.

8. A. Yamada, M. Oasa, H. Nagabuchi and M. Kawashima, Material Lett., 1988. 6(5.6): p. 167-169.

9. Z. L. Liau and D. E. Mull, Appl. Phys. Lett., 1990. 56(8): p. 737-739.

10. Y. O. Lo, R. Bhat, D. M. Hwang, M. A. Koza and T. P. Lee, Appl. Phys. Lett., 1991. 58(18): p. 1961-1963.

11. L. A. Gordon, *et al.*, Electron. Lett., 1993. 29(22): p. 1942-1943.

12. Y. O. Lo. personal communications, 1993.

13. H. K. Kingery, W. D. Brown and D. R. Uhlmann, *Introduction to Ceramics*. 2 ed. 1976, New York: Wiley.

14. J. Rodel and A. M. Glaeser, J. Am. Ceram. Soc., 1990. 73: p. 592-601.

15. J. D. Powers and A. M. Glaeser, J. Am. Ceram. Soc., 1992. 75: p. 2547-2558.

16. J. D. Powers and A. M. Glaeser, J. Am. Ceram. Soc., 1993. 76: p. 2225-2234.

17. T. Nishinaga and K.-I. Cho, Jpn. J. Appl. Phys., Part 2 (Letters), 1988. 27: p. L12-14.

18. S. Y. Chiang and G. L. Pearson, J. Appl. Phys., 1975. 46: p. 2986-2991.

19. S. K. Ghandhi, *VSLI Fabrication Principles- Silicon and Gallium Arsenide*. 2 ed. 1994, New York: Wiley.

20. R. Behrensmeir, H. G. Brion, H. Siethoff, P. Veyssiere and P. Hansen, Mat.Sci. & Eng. A (Structural Materials: Properties, Microstructure and Processing), 1991. A137: p. 173-176.

21. S. Guruswamy, R. S. Rai, K. T. Faber and J. P. Hirth, J. Appl. Phys., 1987. 62: p. 4130-4134.

22. S. Guruswamy, *et al.*, J. Appl. Phys., 1989. 65: p. 2508-2512.

23. C. Chatillon and D. Hatin, J. Cryst. Growth, 1995. 151: p. 91-101.

24. C. T. Foxton, J. A. Harvey and B. A. Joyce, J. Phys. Chem. of Solids, 1973. 34: p. 1693-1701.

25. J. Lagowski, *et al.*, Appl. Phys. Lett., 1986. 49(14): p. 892-894.

26. D. C. Look, *et al.*, Appl. Phys. Lett., 1986. 49(17): p. 1083-1085.

27. O. Oda, *et al.*, Semicond. Sci. Technol., 1992. 7: p. A215-A223.

IX. Publications

1. L. Gordon, G. L. Woods, R. C. Eckardt, R. K. Route, R. S. Feigelson, M. M. Fejer and R. L. Byer, "Diffusion bonded stacked GaAs for quasi-phase-matched second harmonic generation of a carbon dioxide laser," Electron. Lett. 29, pp. 1942-1944 (1993).

   (This publication describes research relevant to the work described here that was supported by the earlier ONR Grant supporting CNOM, N00014-92-J-1903.)

2. L. Gordon, R. C. Eckardt and R. L. Byer, "Investigations of diffusion-bonded quasi-phase-matched GaAs for infrared parametric oscillation," Proc. SPIE 2145, pp. 316-326 (1994).

   (This publication describes research supported in part by the earlier ONR Grant supporting CNOM, N00014-92-J-1903.)

Invited Presentations

R. L. Byer, "Diffusion Bonding of Mid-IR Nonlinear Optical Materials," Materials Research Society, Boston, Maryland (November 30-December 2, 1993).

L. A. Gordon, D. Zheng, Y. C. Wu, R. C. Eckardt, R. K. Route, R. S.Feigelson, M. M. Fejer, and R. L. Byer, "Diffusion-Bonded-Stacked Materials for High Peak and Average Power IR Application," CLEO Pacific Rim Conference, Chiba, Japan (July 11-14, 1995)

Contributed Presentations

L. Gordon, G. L. Woods, R. Route, R. S. Feigelson, R. Eckardt, M. M. Fejer, and R. L. Byer, "Diffusion Bonded Gallium Arsenide Stack of Plates for Quasi Phase Matched Second Harmonic Generation of a Carbon Dioxide Laser," CLEO '93, Baltimore, Maryland (May 2-7, 1993) [Post-Deadline Paper].

L. A. Gordon, R. C. Eckardt, and R. L. Byer, "Investigations of Diffusion-Bonded Quasi-Phase-Matched GaAs for Infrared Parametric Oscillation," Optoelectronic for Information and Microwave Systems (SPIE OE/LASE '94), Paper 2145-44, Los Angeles, California (January 22-29, 1994).

L. A. Gordon, D. Zheng, Y. C. Wu, R. C. Eckardt, R. K. Route, R. S. Feigelson, M. M. Fejer and R.
L. Byer, "Diffusion-bonded stacked GaAs for quasi-phasematched frequency conversion throughout the IR," OSA Annual Meeting, Portland Oregon (September 10-15, 1995).

Contributed Presentations, cont.

D. Zheng, L. A. Gordon, R. C. Eckardt, M. M. Fejer and R. L. Byer, "Diffusion bonding of GaAs wafers for nonlinear optical applications," to be presented at the 189th Meeting of the Electrochemical Society, Los Angeles (May 5-10, 1996).

D. Zheng, L. A. Gordon, R. C. Eckardt, M. M. Fejer and R. L. Byer, "Progress in reducing loss of diffusion bonded stacked GaAs for mid-infrared generation," to be presented at the OSA topical meeting, Nonlinear Optics: Materials, Fundaments and Applications, Maui, Hawaii (July 7-12, 1996).

X. Appendices

A. L. Gordon, G. L. Woods, R. C. Eckardt, R. K. Route, R. S. Feigelson, M. M. Fejer and R. L. Byer, "Diffusion bonded stacked GaAs for quasi-phase-matched second harmonic generation of a carbon dioxide laser," Electron. Lett. 29, pp. 1942-1944 (1993).

B. L. Gordon, R. C. Eckardt and R. L. Byer, "Investigations of diffusion-bonded quasi-phase-matched GaAs for infrared parametric oscillation," Proc. SPIE 2145, pp. 316-326 (1994).

C. D. Zheng, L. A. Gordon, R. C. Eckardt, M. M. Fejer and R. L. Byer, "Diffusion bonding of GaAs Wafers for nonlinear opticas applications," summary of a paper to be presented at the 189th Meeting of the Electrochemical Society, Los Angeles, May 5-10, 1996.

D. D. Zheng, L. A. Gordon, R. C. Eckardt, M. M. Fejer and R. L. Byer, "Progress in reducing loss of diffusion bonded stacked GaAs for mid-infrared generation," summary of a paper submitted fopr presentation at the OSA topical meeting Nonlinear Optics: Materials, Fundaments and Applications, Maui, Hawii, July 7-12, 1996.

Diffusion-bonded stacked GaAs for quasi-phase-matched second-harmonic generation of a carbon dioxide laser

L. Gordon, G.L. Woods, R.C. Eckardt, R.R. Route, R.S. Feigelson, M.M. Fejer and R.L. Byer

Indexing terms: Gallium arsenide, Optical harmonic generation, Gas lasers

The authors have fabricated a diffusion-bonded monolithic stack of GaAs plates for quasi-phase-matched second-harmonic generation of a 10.6μm CO_2 laser. This synthetic nonlinear crystal retains the thermomechanical properties of the bulk material, and has provided phase coherent nonlinear interaction over ~0.4cm.

High average power coherent sources are needed throughout the infra-red and nonlinear frequency conversion of existing lasers can provide these sources. However, currently available infra-red (IR) nonlinear materials (e.g. the chalcopyrites $AgGaS_2$, $AgGaSe_2$, and $ZnGeP_2$) are limited by low surface damage thresholds, large absorption coefficients, or low thermal conductivity [1,2]. GaAs and ZnSe have high thermal conductivities and low absorption coefficients, and are widely used for windows and mirrors in high-power IR laser systems. These cubic crystals also have large second-order nonlinear susceptibilities; however, they cannot be birefringently phasematched, and, therefore, have not been used in practical frequency conversion applications.

An alternative to birefringent phase matching is quasi-phase-matching (QPM) [3,4,5], where a periodic modulation of the nonlinear susceptibility compensates for the phase velocity mismatch between the interacting waves. Stacks of discrete plates at the Brewster angle have been used to quasi-phase-match second-harmonic generation (SHG) in GaAs [6,7] and CdTe [8], but reflection and scattering losses associated with the many interfaces in the air-spaced layers precluded wide-spread application. Although thin plates (250μm) of LiB_3O_5 have been optically contacted with good results [9], the high indices of refraction of III-V semiconductors lead to significant losses for optical contacting wafers with practical polishing tolerances [6].

To eliminate the air-semiconductor interface problems, we diffusion bonded the adjacent layers to create a monolithic structure. Diffusion bonding has previously been used both for joining dissimilar semiconductors for optoelectronic devices [10,11] and for fabricating laser slabs with nonuniform doping [12]. We report here the fabrication and nonlinear optical testing of diffusion-bonded stacked (DBS) GaAs for 10.6 – 5.3μm second-harmonic generation.

A variety of undoped and lightly doped GaAs wafers were used. They were all mechanical grade and polished on both sides. The wafers were diced into 1cm² pieces. The pieces were cleaned thoroughly with trichloroethane, followed by acetone and finally methanol. They were then stacked in a boron nitride holder between graphite spacers. Pressure was applied with a 1kg weight, and the assembled stack was placed in an oven with a 5% H_2 and 95% N_2 atmosphere. The temperature was ramped to 840°C over one hour. After maintaining that temperature for two hours, the oven was cooled to room temperature over approximately eight hours.

Stacks with 2–9 layers were bonded into monolithic units. The samples cleaved along the crystal planes leaving the bonded surfaces intact. We were able to bond wafers regardless of their dopings, their alignment of crystalline axes and their orientations: {100} to {100}, {110} to {110} and {110} to {100}. The exterior surfaces of the stack, which were in contact with the graphite spacers, were noticeably degraded after the processing. We did not repolish these surfaces, as the resulting uncertainty in the layer thicknesses would have hampered analysis of the SHG results.

The {110} wafers were chosen for the SHG studies because they provided the maximum effective nonlinear coefficient in GaAs for propagation normal to the input face. Adjacent wafers were rotated by 180° to alternate the sign of the effective nonlinear coefficient. The dispersion equation [13] predicts a coherence length, L_c, of 106μm for doubling 10.6μm radiation in GaAs. Available {110} wafers were 435μm thick (±5μm). Although this

thickness was adequate for intial testing of the diffusion bonding technique, it was not an odd multiple of L_c and, therefore, not optimal for SHG at 10.6μm.

Five samples, with 2, 3, 5, 7, and 9 layers were characterised, and compared to a single plate. Linearly polarised 10.6μm radiation from a grating-tuned, 200ns, Q-switched CO_2 laser was incident normal to the DBS GaAs sample with approximately 2 MW/cm² peak intensity. Second-harmonic output power at 5.3μm was measured with an InSb detector. The fundamental polarisation was fixed along a <111> direction.

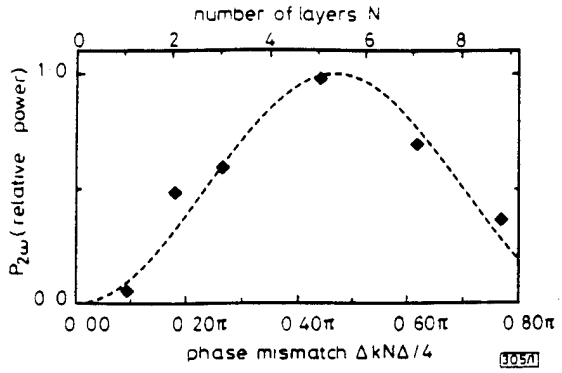

Fig. 1 *Second harmonic output power, $P_{2\omega}$ of CO_2 laser as function of phase mismatch and number of layers in diffusion-bonded quasi-phase-matched GaAs structures*

◆ data
- - - $\sin^2$ fit

Fig. 1 shows the relative SHG power for diffusion bonded stacks of two, three, five, seven and nine layers, as well as for a single plate. The measured thickness of the wafers was used to calculate the total phase mismatch as a function of the number of layers, N, and the output power was compared to the expected $\sin^2(\Delta kN\Lambda/4)$ dependence, where $\Delta k = k_{2\omega} - 2k_\omega - K_m$, and the wave vector due to the QPM grating is $K_m = 2\pi m/\Lambda$. Here k_ω and $k_{2\omega}$ are the wave vectors for the fundamental and second-harmonic frequencies, respectively. The period of the modulation, Λ, is twice the wafer thickness. The integer m is the order of the QPM [5]. The agreement with the expected dependence on the number of layers demonstrates that the DBS GaAs acts as a monolithic structure with a modulated nonlinear coefficient, providing a phase coherent interaction.

Many potential applications of these DBS GaAs structures involve frequency conversion at high average and high peak power. Some preliminary damage measurements were therefore performed. We exposed both the bulk and DBS GaAs to increasingly higher intensities for up to 5 min and then examined the samples under a microscope for damage. A 26W CW CO_2 laser beam was focused to a ~60μm $1/e^2$ radius spot, producing an intensity of ~500kW/cm². No damage was detected, whereas $AgGaSe_2$ damages at 5–60kW/cm² with a CW CO_2 laser [1]. A 1kHz pulsed CO_2 laser with 60 – 500μs pulse width was focused to a peak intensity of 30MW/cm². No damage was seen in the bulk GaAs. We were unable to obtain accurate data from the DBS GaAs at this power level because the degraded outer surfaces developed damage characteristic of thermal runaway. However, the samples were not noticeably damaged with a single pulse, whereas $AgGaSe_2$ is damaged at ~10MW/cm² for 80–180 ns pulsed operations [2].

DBS GaAs has very large acceptance bandwidths due to non-critical phase matching and high index of refraction with low dispersion [13]. For a 1cm long structure for SHG at 10.6μm (~94 layers), the FWHM wavelength acceptance is 0.5μm, and the temperature acceptance is 270°C. The external angular acceptance is 64° FWHM. Because GaAs is not birefringent, there is no birefringent walk-off at any incidence angle, and QPM produces no phase-velocity walk-off at normal incidence [5].

Variations on the basic structure can be fabricated. Fig. 2*b* shows a structure with {100} oriented cap layers. For this orientation there is no effective nonlinear coefficient at normal incidence. Because the thickness of these cap layers is not important, this structure could be repolished, without compromising the conversion efficiency. QPM allows novel designs not possible with birefringent phase matching. For example, the structure shown in Fig. 2*c*, composed of wedged wafers, allows wavelength tuning by translation instead of by rotation. Caps could be added to this structure eliminating any overall linear wedge, thus avoiding beam steering effects. Such structures would be particularly useful for mid-IR optical parametric oscillators and mixers.

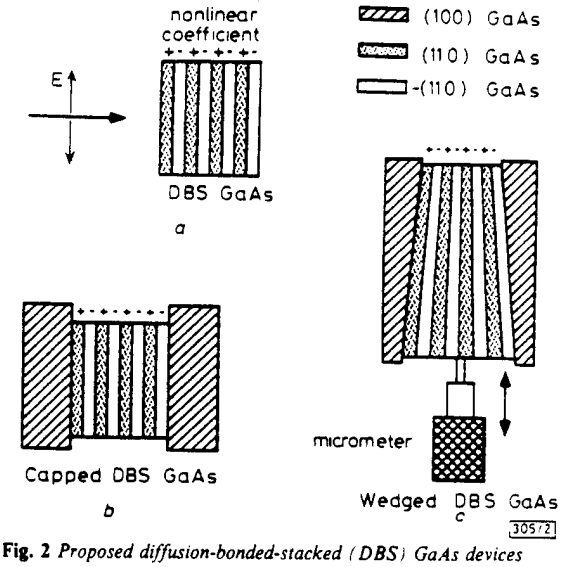

Fig. 2 *Proposed diffusion-bonded-stacked (DBS) GaAs devices*

a Basic DBS GaAs structure that was fabricated and tested
b Basic structure with {100} GaAs cap
c Wedged DBS GaAs structure which allows wavelength tuning by translation

These preliminary results indicate the feasibility of fabricating DBS structures. We were able to fuse wafers to form monolithic crystals, with bond strengths comparable to the bulk material. We measured SHG nonlinear conversion which followed theoretical predictions. We also determined that the damage thresholds are at least 500kW/cm² for CW and 30 MW/cm² for peak power at 10.6μm. Current work includes polishing the layers to the correct thicknesses, and repolishing the devices after processing, increasing the numbers of layers to improve conversion efficiency and testing for damage thresholds at different wavelengths, and with higher power lasers. In the future, the DBS processing techniques may be extended to other nonlinear crystals such as ZnSe to take advantage of different material characteristics, and to other applications such as difference frequency generation or parametric devices for tunable infrared generation.

Acknowledgments: We wish to thank D. Smith of Coherent Inc. for help with the damage measurements and L. Randall for assistance with mechanical design and fabrication. This work was supported by US Army Research Office contract DAAL03-92-G-0400, and Office of Naval Research grant NOOO14-92-J-1903.

27 August 1993
Electronics Letters Online No: 19931233

L. Gordon, G. L. Woods, R. C. Eckardt, R. R. Route, R. S. Feigelson, M. M. Fejer and R. L. Byer (*Center for Nonlinear Optical Materials, Stanford University, Stanford, CA 94305, USA*)

References

1 ACHAREKAR, M., MONTGOMERY, J., and RAPP, R.: 'Laser damage threshold measurements of $AgGaSe_2$ at 9μm'. Proc. of Boulder Damage Symp., NIST Boulder CO, 1991, (USA)

2 ZIEGLER, B.C., and SCHEPLER, K.L.: 'Transmission and damage-threshold measurements in $AgGaSe_2$ at 2.1μm', *Appl. Opt.*, 1991, **30**, pp. 5077–5080

3 ARMSTRONG, J.A., BLOEMBERGEN, N., DUCUING, J., and PERSHAN, P.S.: 'Interactions between light waves in a nonlinear dielectric', *Phys. Rev.*, 1962, **127**, pp. 1918–1939

4 MCMULLEN, J.D.: 'Optical parametric interactions in isotropic materials using a phase-corrected stack of nonlinear dielectric plates', *J. Appl. Phys.*, 1975, **46**, pp. 3076–3081

5 FEJER, M.M., MAGEL, G.A., JUNDT, D.H., and BYER, R.L.: 'Quasi-phase-matched second harmonic generation: Tuning and tolerances', *IEEE J. Quantum Electron.*, 1992, **28**, pp. 2631–2654

6 SZILAGYI, A., HORDVIK, A., and SCHLOSSBERG, H.: 'A quasi-phase-matching technique for efficient optical mixing and frequency doubling', *J. Appl. Phys.*, 1976, **47**, pp. 2025–2032

7 THOMPSON, D.E., MCMULLEN, J.D., and ANDERSON, D.B.: 'Second-harmonic generation in GaAs "Stack of Plates" using high-power CO_2 laser radiation', *Appl. Phys. Lett.*, 1976, **29**, pp. 113–115

8 PILTCH, M.S., CANTRELL, C.D., and SZE, R.C.: 'Infrared second harmonic generation in nonbirefringent cadmium telluride', *J. Appl. Phys.*, 1976, **47**, pp. 3514–1517

9 MAO, H., FU, F., WU, B., and CHEN, C.: 'Noncritical quasiphase-matched second harmonic generation in LiB_3O_5 crystal at room temperature', *Appl. Phys. Lett.*, 1992, **61**, pp. 1148–1150

10 LIAU, Z.L., and MULL, D.E.: 'Wafer fusion: A novel technique for optoelectronic device fabrication and monolithic integration', *Appl. Phys. Lett.*, 1990, **56**, pp. 737–739

11 LO, Y.O., BHAT, R., HWANG, D.M., KOZA, M.A., and LEE, T.P.: 'Bonding by atomic rearrangement of InP/InGaAsP 1.5mm wavelength lasers on GaAs substrates', *Appl. Phys. Lett.*, 1991, **58**, pp. 1961–1963

12 LEE, H.C., BROWNLIE, P.A., MEISSNER, H.E., and REA, E.C.: 'Diffusion bonded composites of YAG single crystals'. Proc. SPIE, 1991, pp. 2–10

13 PIKHTIN, A.N., and YAS'KOV, A.D.: 'Dispersion of the refractive index of semiconductors with diamond and zinc-blende structures', *Sov. Phys. Semicond.*, 1978, **12**, pp. 622–626

Investigations of diffusion-bonded stacked GaAs for infrared quasi-phasematched parametric oscillation

L. A. Gordon, R. C. Eckardt and R. L. Byer

Center for Nonlinear Optical Materials
Stanford University, Stanford, CA, 94305

ABSTRACT

We are developing the diffusion-bonded stacked (DBS) structure for quasi-phasematched interactions to meet the need for high power nonlinear conversions in the infrared. In our preliminary investigations, we have compared optical and thermal properties of some potential DBS materials. Theoretical projections of device performance were compared for DBS GaAs and ZnSe and birefringent crystals $ZnGeP_2$ and $AgGaSe_2$ for both second-harmonic generation (SHG) of 10-μm radiation and 2-μm pumped optical parametric oscillators (OPO's). We are refining bonding processes for GaAs and have initial diffusion bonding results for ZnSe. We have fabricated and tested DBS GaAs structures for SHG, demonstrating that the crystal orientation is conserved during the bonding process, and that the nonlinear generation of the individual layers sums coherently. These studies indicate that DBS materials have potential for application in high-average-power OPO's.

1. INTRODUCTION

High-average-power coherent sources are needed throughout the infrared, especially in the 3 to 5-μm region. Nonlinear frequency conversion of existing lasers can provide these sources. Optical parametric oscillators (OPO's) are attractive nonlinear devices because they can provide output tunable over a wide range; however, currently available infrared (IR) nonlinear materials, e.g. the chalcopyrites $AgGaS_2$, $AgGaSe_2$, and $ZnGeP_2$, are limited by low surface damage thresholds, large absorption coefficients, or low thermal conductivity[1,2]. GaAs and ZnSe have high thermal conductivities and low absorption coefficients, and are widely used for windows and mirrors in high power IR laser systems. These cubic crystals also have large second order nonlinear susceptibilities; however, they cannot be birefringently phasematched, and, therefore, have not been used in practical frequency conversion applications.

An alternative to birefringent phasematching is quasi phasematching (QPM)[3,4,5], where a periodic modulation of the nonlinear susceptibility compensates for the phase velocity mismatch between the interacting waves. Stacks of discrete plates at Brewster angle have been used to quasi phasematch second harmonic generation (SHG) in GaAs[6,7] and CdTe[8], but reflection and scattering losses associated with the many interfaces in the air-spaced layers precluded wide-spread application.

To eliminate the air-semiconductor interface problems, we diffusion bonded adjacent layers of GaAs. Diffusion-bonded stacked (DBS) GaAs devices were fabricated, and SHG of 10.6 μm has been demonstrated[9,10]. Our goal now is the demonstration of a DBS optical parametric oscillator (OPO). We have investigated the different elements necessary in the realization of a mid infrared DBS OPO, and report on the progress in theory, bonding, devices and nonlinear testing.

2. QUASI PHASEMATCHING

QPM is achieved by a periodic modulation of the nonlinear susceptibility which compensates for the phase velocity mismatch between the interacting polarization waves, allowing efficient interactions in the absence of phase-velocity matching. Optimally, the modulation of the nonlinear susceptibility is a sign reversal, with a period Λ equal to twice the coherence length, L_c. The coherence length is the distance over which a π phase difference develops between the fundamental and the harmonic polarization waves, and is related to $\Delta k'$, the wave vector mismatch due to material dispersion, by

$$L_c = \pi/\Delta k', \qquad \text{where} \qquad \Delta k' \equiv k_1 - k_2 - k_3 = (n_1\omega_1 - n_2\omega_2 - n_3\omega_3)/c,$$

n is the refractive index, k is the wave vector, c is the speed of light in vacuum, and subscripts refer to quantities evaluated at the three interacting frequencies; we use the convention $\omega_1 > \omega_2 \geq \omega_3$. For efficient QPM, one of the spatial harmonics $K_m = 2\pi m/\Lambda$ of the periodically modulated medium must lie close to $\Delta k'$, where m is an integer and is the order of the quasi

0-8194-1440-9/94/$6.00

phasematching. If this condition holds, quasi-phasematched nonlinear interactions behave similarly to conventionally phasematched nonlinear interactions, but with an effective wave vector mismatch $\Delta k = \Delta k' - K_m$, and an effective nonlinear susceptibility d_m equal to the amplitude of the mth Fourier component of the nonlinear susceptibility. For odd-order QPM (m = 1, 3, 5 ...) with 50% duty cycle, $d_m = 2d_{eff\text{-}b}/m\pi$, where $d_{eff\text{-}b}$ is the effective nonlinear coefficient for the homogeneous bulk material. Detailed analyses of QPM appear in Refs.[4,5,11].

Developing appropriate means to periodically modulate the nonlinear susceptibility is the limiting step for practical devices for QPM interactions. Typical coherence lengths in the visible are several microns and in the IR are several tens to hundreds of microns. Success in the creation of periodic domain structures in bulk and thin film oxide ferroelectrics has led to rapid progress in QPM for visible and near IR interactions (see Refs. in [5]), but the transparency range of these materials precludes their use in the mid IR and far IR. Techniques for patterning the orientation of semiconductor films are emerging[12]; however, thin films are limited in their power handling capabilities. At present the only technique for producing bulk quasi-phasematched semiconductor media appears to be stacking rotated crystal plates. DBS structures permit the reduction of losses below those observed for air-spaced plates. While thin plates (250-μm) of LiB_3O_5 have been optically contacted with good results for QPM interactions[13], the high indices of refraction of III-V semiconductors lead to significant losses for optical contacting wafers with practical polishing tolerances[6].

3. PRACTICAL DEVICES

The established high power lasers in the infrared are: Neodynium at 1 μm, and CO_2 at 10 μm. Holmium and Thulium based lasers are also being developed at 2 μm. There exists a variety of semiconductor lasers from 0.8 to 1.5 μm; however, their current lower powers prevents their use in high conversion nonlinear applications. We have identified options to produce wavelengths in the 3-5 μm region working from these sources: a 10-μm pumped SHG, a 1-μm pumped OPO, a 1-μm pumped OPO which then pumps a difference frequency generator (DFG) or OPO, and a 2-μm pumped OPO. Each of these devices utilizes DBS materials. SHG is simple to demonstrate; however, the resulting wavelengths are limited by existing sources. Similarly, DFG demonstration is also relatively simple, but limited for wavelengths unless pumped by an OPO. OPO's can provide an enormous range of wavelengths; however, gain and loss is critical. There must be sufficient gain to allow the OPO to reach threshold during the pulse for a pulsed pump, or the loss must be low enough to permit the OPO to reach threshold below the damage threshold of the crystal in the continuous regime. The first DBS OPO demonstrated will probably be a singly resonant OPO (SRO) in the pulsed regime. Different types of three-wave nonlinear interactions are listed in Table 1. The waves are identified by frequency.

Table 1. Nonlinear Devices

input	output	interaction	device
ω_2 , ω_3	ω_1	$\omega_2 + \omega_3 = \omega_1$	Sum Frequency Generator (SFG)
ω_2	ω_1	$\omega_2 + \omega_2 = \omega_1$	Second Harmonic Generator (SHG)
ω_1	ω_2 , ω_3	$\omega_1 = \omega_2 + \omega_3$	Optical Parametric Oscillator (OPO)
ω_1 , ω_2	ω_3	$\omega_1 - \omega_2 = \omega_3$	Difference Frequency Generator (DFG)
ω_1 , ω_3	ω_2	$\omega_1 - \omega_3 = \omega_2$	

We need to produce both fixed wavelength and tunable sources. QPM tunability can be achieved in three different ways. As with birefringent crystals, DBS structures may be tuned by temperature and angle; however, this only provides coverage over narrow-spectral regions. DBS crystals may also be fabricated with intrinsic tunability. If the layers are wedged, the crystal may be tuned by translating it perpendicular to the incident beam, thus increasing or decreasing the coherence length. The wedged structure may provide greater tuning range than either angle or temperature tuning, and it does not introduce alignment problems such as those associated with rotating the crystal.

There are many developmental stages in the realization of a DBS OPO. We need to choose a material with appropriate optical characteristics, develop a diffusion bonding process for that material, fabricate a device with modulated nonlinear domains and verify that we do not degrade the domain orientation or the crystal quality during the fabrication process, demonstrate nonlinear conversion for SHG and DFG, and finally demonstrate nonlinear conversion for parametric oscillation and amplification where low loss is critical.

3.1 Materials

Useful DBS materials must have low absorption for the interaction frequencies, and have an adequate nonlinear coefficient. They need to be diffusion bondable, and have a workable coherence length for the desired interaction. For high peak power and high average power, the crystals need a high damage threshold and large thermal conductivity, respectively.

Table I compares the optical and thermal properties of III-V and II-VI semiconductors. Values for many of the properties, ie. nonlinear coefficient and absorption, vary by factors of three or more depending on the references. We have chiefly used four different references[14,15,16,17] comparing the results obtained for the same materials.

Table 2. Properties of some nonlinear semiconductors

properties	GaAs	GaP	InSb	InAs	InP	ZnSe	β-ZnS
nonlinear coefficient (d_{14}) (pm/V)	83 [14]	37 [14]	500 [15]	300 [15]	140 [15]	50 [15]	25 [15]
transmission range (μm)	1-16	0.6-11	8-25	3.8-7	1-14	0.5-22	1-11
dn/dT (°K) @ 10 μm	1.5×10^{-4}	1.0×10^{-4}	1.5×10^{-4}	2.9×10^{-4}	8.2×10^{-5}	6.8×10^{-5}	4.1×10^{-5}
(1/L)dL/dT ($°K^{-1}$)	5.7×10^{-6}	5.3×10^{-6}	5.0×10^{-6}	5.3×10^{-6}	4.5×10^{-6}	7.0×10^{-6}	6.7×10^{-6}
Thermal conductivity K (W/m°K)	52	110	36	50	70	18	27
n @10μm	3.27	2.96	3.95	3.42	3.05	2.41	2.20
α (cm^{-1}) @10μm	0.01	0.21	0.009	20	<0.1	0.0005	0.15

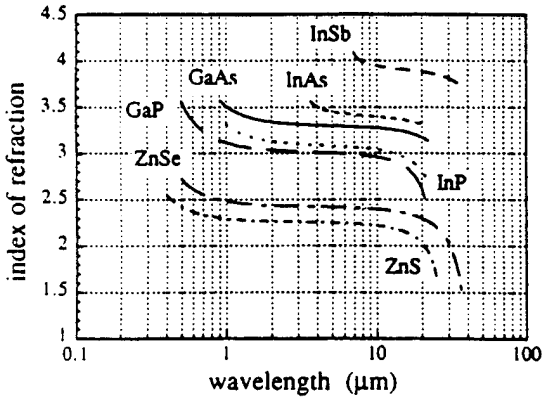

Figure 1. Dispersion curves for III-V and II-VI semiconductor materials.

The ideal material will depend on the application. The dispersion properties of some potential DBS materials are shown in Figure 1. These curves were generated using dispersion equations given by Pikhtin and Yas'kov[18]. The regions of low dispersion near the center of the curves indicate the useful spectral region for that material. The flatter the dispersion curve, the longer the coherence length, and the fewer bonds necessary for a given length of crystal. The coherence lengths for different nonlinear interactions determine the feasibility of the DBS structure. The longer the L_c, the easier the wafer is to polish and handle, and the more tolerent the final device is to absolute thickness errors.

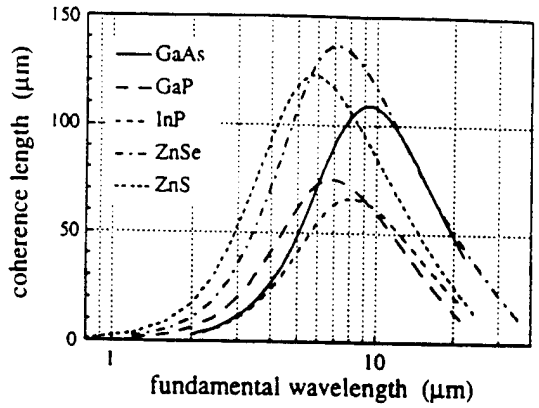

Figure 2. Coherence lengths for second harmonic generation of the mid IR in GaAs, GaP, InP, ZnSe, and ZnS.

Coherence lengths for SHG, calculated from the dispersion relationships, are shown as a function of fundamental wavelength in Figure 2. The materials GaAs, ZnSe, and ZnS are of particular interest because of their longer coherence lengths.

Figures 3 and 4 show calculated tuning curves for difference frequency generation (DFG) in DBS GaAs and ZnSe. These tuning curves are more complicated than those for SHG because it is necessary to specify two input wavelengths for DFG. Here we assume that the input waves for DFG are the signal and the idler generated in an OPO pumped at 1.064 μm. The signal and the idler wavelengths are designated by λ_s and λ_i. The output wavelength from the DFG is λ_d. Because the coherence lengths are short, these devices would be more easily fabricated for third order QPM.

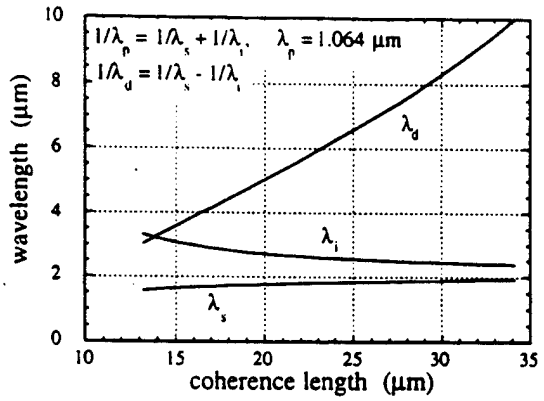

Figure 3. Difference frequency generation in DBS GaAs for mixing the signal and idler from a 1.06-μm-pumped OPO. The output wavelength, λ_d, vs the coherence length is shown.

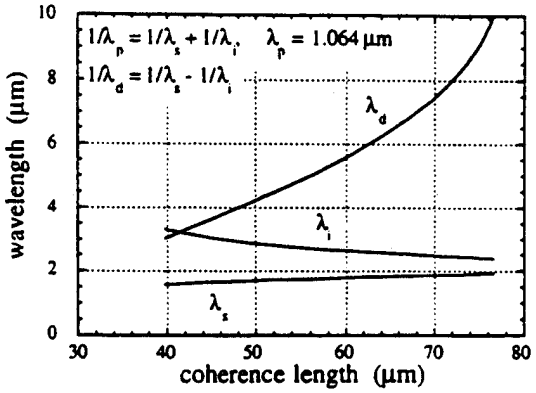

Figure 4. Difference frequency generation, λ_d, for DBS ZnSe when pumped by the signal and idler from a 1.06-μm-pumped OPO.

For shorter wavelengths, approaching 1-μm, the dispersion increases for most of the semiconductors, and the coherence lengths decrease making it more difficult to fabricate devices; therefore, we have considered only the 2-μm pumped OPO option which we present in Figures 5 and 6. For these calculations, we have asssumed that the DBS OPO's are pumped by the output of a 1-μm pumped OPO operating at degeneracy.

We selected GaAs for the initial demonstration, because GaAs has the lowest absorption over the widest transmission window apart from ZnSe, and because inexpensive high-quality single-crystal wafers are commercially available. Although ZnSe shows promise due to it's very low absorption, single crystal ZnSe is only now becoming available and is still very expensive.

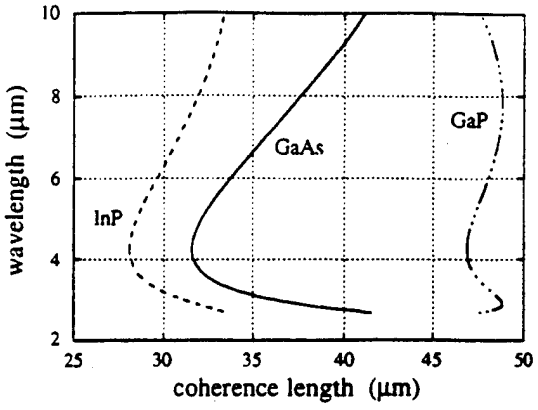

Figure 5. Parametric oscillator tuning curves for III-V semiconductor compounds for a 2.13-μm pump wavelength.

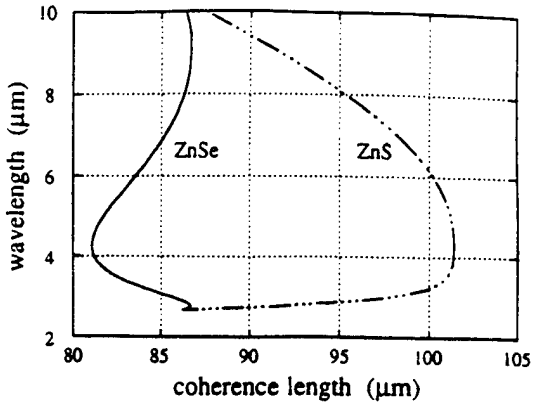

Figure 6. Parametric oscillator tuning curves of II-VI compounds ZnSe and ZnS. The low absorption loss of ZnSe may allow very high average power parametric oscillator devices when pumped at 2.13 μm.

3.2 Diffusion Bonding

Diffusion bonding enables permanent bonding between surfaces without disturbing the crystalline structure, and without introducing another material (i.e. glue) between the surfaces. Adjacent surfaces are brought into close contact under pressure, and heated in an appropriate atmosphere to allow diffusion across the interface, creating a monolithic structure which is stable when exposed to thermal gradients (unlike optical contacting) and essentially indistinguishable from a bulk crystal. Diffusion bonding has previously been used both for joining dissimilar semiconductors for optoelectronic devices[19,20,21,22,23,24], and for fabricating laser slabs with nonuniform doping[25,26]. For a DBS crystal there is ideally no difference in linear optical properties between the bond and the bulk material, nor any change of index of refraction at the interfaces.

There are two different mechanisms or stages in diffusion bonding. The first is the diffusion process: two surfaces are placed very closely together permitting electrons and atoms to move from one surface to the other. This process is not dependent on pressure, but is dependent on temperature and time. The atoms cannot move unless there are adjacent vacancies, and they are equally likely to diffuse in any direction. The second stage involves mass transport. The wafer is deformed by pressure to force all the surfaces into contact. The point at which this deformation occurs is called the yield point, and depends on temperature, pressure, and the number of dislocations[27]. This deformation will increase the stress, and the number of dislocations in the crystal. It is not yet known how this will affect the optical properties of a DBS structure.

We have experimentally diffusion bonded a variety of undoped and lightly doped GaAs wafers. They were all mechanical grade and polished on both sides. The wafers were diced into 1-cm^2 pieces. The pieces were cleaned thoroughly with trichloroethane, followed by acetone and finally methanol; they were then stacked in a boron nitride holder between graphite spacers. Pressure was applied with a 1-kg weight, and the assembled stack was placed in an oven with a 5% H_2 and 95% N_2 atmosphere. The temperature was ramped to 840° C over 1 hour. After maintaining that temperature for two hours, the oven was cooled to room temperature over approximately 8 hours.

Stacks with 2 through 9 layers were bonded into monolithic units. The samples cleaved along the crystal planes leaving the bonded surfaces intact. We were able to bond wafers regardless of their dopings, their alignment of the crystalline axes, and their orientations: {100} to {100}, {110} to {110} and {110} to {100}. The exterior surfaces of the stack, which were in contact with the graphite spacers, were noticeably degraded after the processing. We did not repolish these surfaces, as the resulting uncertainty in the layer thicknesses would have hampered analysis of the SHG results.

We have succeeded in diffusion bonding polycrystalline ZnSe under similar conditions to GaAs. We expect polycrystals and single crystals to have similar bonding characteristics. When single crystal ZnSe growth is better

characterized, we will be able to transfer the DBS technology developed for GaAs to ZnSe. The key parameters in diffusion bonding are: surface preparation, applied pressure, temperature and time. We are currently studying the quality of the bonds as a function of these parameters. By considering the melting points, vapor pressures, surface mobilities and yield points, we should be able to transfer bonding processes from one compound to another.

3.3 DBS Nonlinear Structure

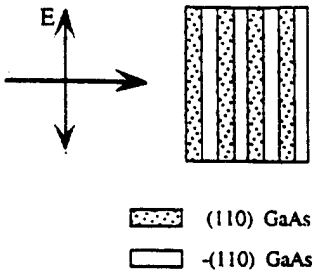

Figure 7. Basic DBS Structure in GaAs showing the layers of alternating nonlinear coefficients

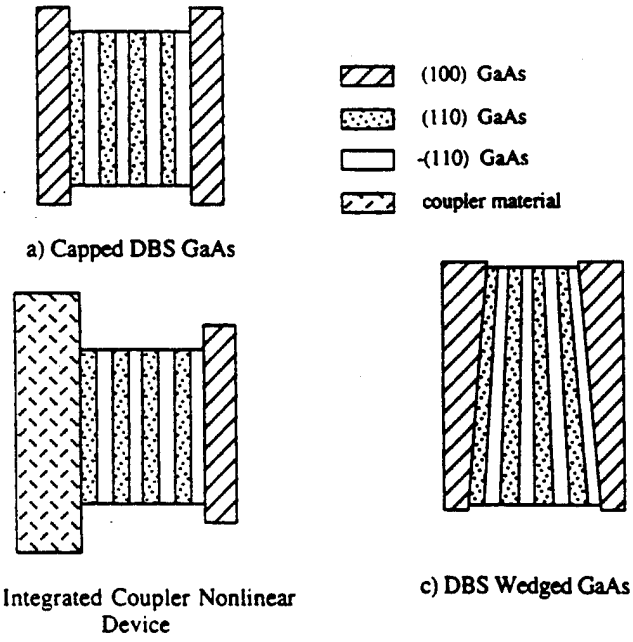

Figure 8. Variations on DBS structure in GaAs

Both GaAs and ZnSe are $\bar{4}3m$ crystals where the maximum nonlinear coefficient is for radiation polarized along a <111> direction. The {110} wafers were chosen for the nonlinear studies because they provide the maximum effective nonlinear coefficient for propagation normal to the input face. Adjacent wafers were rotated by 180° to alternate the sign of the effective nonlinear coefficient.

Figure 7 shows a schematic of the basic DBS structure. Figure 8a shows a structure with {100} oriented cap layers. For this orientation, there is no effective nonlinear coefficient at normal incidence. Since the thickness of these cap layers is not important, this structure could be repolished, without compromising the conversion efficiency. The DBS structure can be built into laser output couplers, as shown in Figure 8b. This would reduce interface loss. This configuration would be especially suited to SHG of a CO_2 laser, because the DBS structure could be made of the single crystal version of the polycrystalline coupler material. Figure 8c shows the wedged DBS structure which allows wavelength tuning by translation instead of by rotation. Caps could be added to this structure eliminating any overall linear wedge, thus avoiding beam steering effects. The wedged DBS structure would permit larger tuning regions than comparable birefringent crystals because the incident beam remains normal to the crystal at all times. Such structures would be particularly useful for optical parametric oscillators and mixers. We have fabricated both the basic structure and the capped DBS structure.

The DBS structure has a number of benefits compared to birefringently phasematched nonlinear crystals. DBS GaAs has very large acceptance bandwidths due to noncritical phasematching and high index of refraction with low dispersion [18]. For a 1-cm-long DBS GaAs structure for SHG at 10.6-μm (~94 layers), the FWHM wavelength acceptance is 0.5-μm, and the temperature acceptance is 270°C. The external angular acceptance is 64° FWHM. Since GaAs is not birefringent, there is no birefringent walk-off at any incidence angle, and QPM produces no phase-velocity walkoff at normal incidence [5]

3.4 Nonlinear Devices: Predictions

It is useful to compare the theoretical projections of potential DBS materials such as GaAs and ZnSe to those of established birefringent nonlinear crystals such as $ZnGeP_2$ and $AgGaSe_2$. These comparisons are presented give indications of material performance under similar conditions. If we disregard absorption, which is appropriate for pulsed operation, we obtain figures of merit that are the same order of magnitude for all the materials considered. However, absorption and thermal properties must be considered for high-repetition-rate and continuous operation. In these cases, the appropriate figures of merit indicate that the DBS materials are noticably better than the birefringent crystals. $ZnGeP_2$ and $AgGaSe_2$ are both type I phasematched. The "e" and "o" signify the polarizations of the waves in the birefringent crystals, extraordinary and ordinary respectively.

Table 3. Second Harmonic Generation of 10.6-μm radiation in a 1 cm crystal

crystal	transmission range (μm)	d (pm/V)	α (cm^{-1})	K_{therm} (W/mK)	$dn/dT \cdot 10^6$ (K^{-1})	$d\Delta n/dT \cdot 10^6$ (K^{-1})	n_ω	$n_{2\omega}$	ρ (degrees)
GaAs DBS	0.9-12	83	0.01	52	149	1.6	3.271	3.296	-
ZnSe DBS	0.5-14	50	0.0005	18	64	0.7	2.403	2.429	-
$ZnGeP_2$	0.7-12	70	1	35	150 (n_o) 170 (n_e)	20	3.125 (e)	3.125 (o)	-
$AgGaSe_2$	0.7-12	33	0.01	1	70 (n_o) 40 (n_e)	30	2.592 (o)	2.592 (e)	0.68

crystal	θ_{pm} (degrees)	d_{eff} (pm/V)	Δλ (μm)	$\Delta\Theta_{ext}$ (degrees)	ΔT (K)	FOM_{cw}	FOM_p	FOM_{od}	FOM_{hp}
GaAs DBS	-	61	0.48	64	270	6500	2.5	160	3100
ZnSe DBS	-	37	0.2	38	<500	2400000	2.4	2400	33000
$ZnGeP_2$	90 @ T=92°C	70	0.06	41	16	1	3.8	n_e=1.0	2.4
$AgGaSe_2$	55	27	0.12	2	16	2600	1	n_o=6.9	1

d - nonlinear coefficient of the crystal
α - absorption coefficient of the crystal
K_{therm} - thermal conductivity of the crystal
dn/dT - change in index of refraction as a function of temperature; the birefringent crystals have two different indices of refraction
dΔn/dT - $-\Delta n = n_2 - n_1$: change in the difference of index of refraction as a function of temperature
n_ω - index of refraction at 10.6 μm
$n_{2\omega}$ - index of refraction at 5.3 μm

ρ - walkoff angle
Θ_{pm} - phasematching angle measured from the optical axis. DB-QPM structures have no optical axis
d_{eff} - effective nonlinear coefficient taking into account the angle of propagation and quasi phasematching
Δλ - the acceptance bandwidth for wavelengths
$\Delta\Theta_{ext}$ - the acceptance bandwidth for angles (this is the external angle incident on the crystal)
ΔT - the acceptance bandwidth for temperatures

NB. for Figures of Merit. They have all been normalized to the lowest value.

FOM_{cw} -Figure of Merit for a continuous laser: $= d_{eff}^2/n^3\alpha^2$
FOM_p -Figure of Merit for a pulsed laser: $= d_{eff}^2/n^3$
FOM_{od} -Figure of Merit for optical distortion: $= K_{therm}/\alpha dn/dT$
FOM_{hp} -Figure of Merit for high average power performance: $= d_{eff}^2 K_{therm}/\alpha n^2 d\Delta n/dT$

Calculated singly resonant OPO (SRO) thresholds provide another comparison of materials. Table 4. presents the values that were used for the different material parameters. The threshold for the DBS GaAs SRO was calculated assuming both first and third order QPM; first order QPM was assumed for the threshold calculation for ZnSe. Threshold pump pulse energy was calculated using the analysis of Brosnan and Byer[28], with threshold defined as the level of pumping at which the signal output reaches 100 μJ. Both birefringent crystals, $ZnGeP_2$ and $AgGaSe_2$, were type I phasematched. Pump absorption was included. An output coupler of R = 80% was assumed.

Table 4. Values used to calculate the SRO thresholds

crystal	α_p @ 2 μm (cm^{-1})	α_{si} @ 4 μm (cm^{-1})	n_p (2 μm)	n_{si} (4 μm)	θ_{pm} (degrees)	L_c (μm)	Λ (μm)	d_{eff} (pm/V)	ρ (degrees)
GaAs	0.01	0.01	3.341	3.304	-	26.9	53.7	61	-
DBS							161.1	20	
ZnSe	0.002	0.0015	2.435	2.421	-	71.8	143.5	36	-
DBS									
$ZnGeP_2$	0.3	0.02	3.153 (o)	3.153 (e)	56	-	-	64	0.65
$AgGaSe_2$	0.10	0.01	2.619 (e)	2.619 (o)	52	-	-	26	0.64

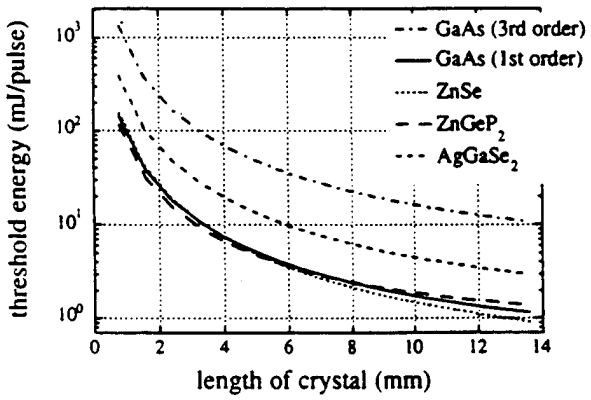

Figure 9. Calculated threshold pulse energies for 2-μm pumped 10-ns pulsed SRO's at degeneracy. The cavity length was 15 mm.

In Figure 9 we compare the calculated threshold pulse energies for degenerate SRO's of DBS GaAs, DBS ZnSe, $ZnGeP_2$ and $AgGaSe_2$. The SRO's are pumped by 10-ns 2-μm pulses. Thresholds of all crystals are within an order of magnitude. As the length of the crystal increases, the absorption becomes more important.

It is important to recall that damage thresholds and average power capabilities will be better for the DBS materials. This will allow superior OPO performance at higher levels of pumping. It should be noted that we have used bulk absorption for GaAs and ZnSe. This assumes no scattering or absorption due to the diffusion bonding. We have not yet shown this experimentally.

3.5 Nonlinear Devices: Experimental

The preliminary nonlinear testing of DBS GaAs used SHG of CO_2 laser radiation. The dispersion equation[18] predicts a coherence length, L_c, of 106 μm for doubling 10.6 μm radiation in GaAs. Available {110} wafers were 435 μm thick (± 5 μm). While this thickness was adequate for intial testing of the diffusion bonding technique, it was not an odd multiple of L_c and, therefore, not optimal for SHG at 10.6 μm.

Five samples, with 2, 3, 5, 7, and 9 layers were characterized, and compared to a single wafer. Linearly polarized 10.6-μm radiation from a grating-tuned, 200-ns, Q-switched CO_2 laser was incident normal to the DBS GaAs sample with approximately 2-MW/cm^2 peak intensity. Second harmonic output power at 5.3 μm was measured with an InSb detector. The SHG power for normal incidence of the fundamental was measured as a function of the angle Φ between the polarization

of the fundamental and the <110> direction. The expected $(1 + 3\sin^2\Phi)\cos^2\Phi$ dependence of the output power was observed. For the remainder of the measurements, the fundamental polarization was fixed along a <111> direction.

Figure 10 shows the relative SHG power for diffusion bonded stacks of 2, 3, 5, 7, and 9 layers, as well as for a single plate. The measured thickness of the wafers was used to calculate the total phase mismatch as a function of the number of layers, N, and the output power was compared to the expected $\sin^2(\Delta k N \Lambda/4)$ dependence, where $\Delta k \equiv k_1 - 2k_2 - K_m$. Here k_2 and k_1 are the wave vectors for the fundamental and second harmonic frequencies, respectively. The period of the modulation, Λ, is twice the wafer thickness. The agreement with the expected dependence on the number of layers demonstrates that the DBS GaAs acts as a monolithic structure with a modulated nonlinear coefficient, providing a phase coherent interaction.

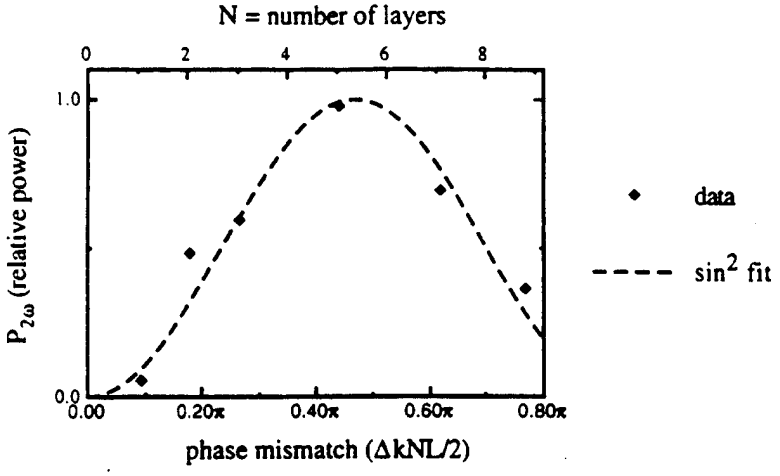

Figure 10. Second harmonic output power, $P_{2\omega}$, of a CO_2 laser as a function of phase mismatch and number of layers in the diffusion-bonded quasi-phasematched GaAs structures.

4. DAMAGE TESTING

Many potential applications of these DBS GaAs structures involve frequency conversion at high average and high peak power; therefore, some preliminary damage measurements were performed. We exposed the both bulk and DBS GaAs to increasingly higher intensities for up to 5 minutes, then examined the samples for damage under a microscope. A 26-W cw CO_2 laser beam was focused to a ~60-μm $1/e^2$ radius spot, producing an intensity of ~500 KW/cm^2. No damage was detected, whereas $AgGaSe_2$ damages at 5-60 KW/cm^2 with a cw CO_2 laser[1]. A 1-kHz pulsed CO_2 laser with 60 to 500-μs pulse width was focused to a peak intensity of 30 MW/cm^2. No damage was seen in the bulk GaAs. We were unable to get accurate data from the DBS GaAs at this power level because the degraded outer surfaces developed damage characteristic of thermal runaway; however, the samples were not noticably damaged with a single pulse, compared to $AgGaSe_2$, which damages at ~10 MW/cm^2 for 80-180 ns pulsed operation[2]. Previous work in this lab has found GaAs wafers to damage at ~300 MW/cm^2 for a 200ns pulse.

5. CONCLUSIONS

Our preliminary investigations of DBS GaAs have included numerical modeling, process development, SHG, and measurement of optical damage characteristics. These results indicate the feasibility of fabricating DBS structures.We chose GaAs for the initial work, and were able to fuse wafers to form monolithic crystals with bond strengths comparable to the bulk material. We measured SHG nonlinear conversion which followed theoretical predictions. We also determined that GaAs damage thresholds are at least 500 kW/cm^2 for cw and 30 MW/cm^2 for peak power at 10.6 μm. These measurements and analyses have demonstrated the potential of high average power OPO operation with this material.

Before we can fabricate a working DBS OPO, we need to expand our work in certain areas: a) we are studying the bonding process. Understanding the mechanisms will permit us to improve the bonds and transfer the technology to other materials. b) we have developed a polishing facility which will allow us to polish the wafers to precise thicknesses and to repolish the ends after processing. c) we need to increase the numbers of layers to improve conversion efficiency. d) we also need to measure damage thresholds at different wavelengths, and with higher power lasers before we can accurately predict maximum operating intensities for the DBS devices.

ACKNOWLEDGEMENTS

We wish to thank D. Smith of Coherent Inc. for help with the damage measurements and L. Randall for assistance with mechanical design and fabrication. This work was supported by U. S. Army Research Office contract DAAL03-92-G-0400, and Office of Naval Research grant NOOO14-92-J-1903.

REFERENCES

1. M. Acharekar, J. Montgomery and R. Rapp, "Laser Damage Threshold Measurement of $AgGaSe_2$ at 9 μm," in proceedings Boulder Damage Symposium, NIST, Boulder, CO, 1991.

2. B. C. Ziegler and K. L. Schepler, "Transmission and Damage-Thresholds Measurements in $AgGaSe_2$ at 2.1 μm," *Appl. Opt.*, vol. 30, no. 34, pp. 5077-5080, Dec. 1991.

3. J. A. Armstrong, N. Bloembergen, J. Ducuing and P. S. Pershan, "Interactions Between Light Waves in a Nonlinear Dielectric," *Phys. Rev.*, vol. 127, no. 6, pp. 1918-1939, Sep. 1962.

4. J. D. McMullen, "Optical Parametric Interactions in Isotropic Materials Using a Phase-Corrected Stack of Nonlinear Dielectric Plates," *J. Appl. Phys.*, vol. 46, no. 7, pp. 3076-3081, Jul. 1975.

5. M. M. Fejer, G. A. Magel, D. H. Jundt and R. L. Byer, "Quasi-Phase-Matched Second Harmonic Generation: Tuning and Tolerances," *IEEE J. Quantum Electron.*, vol. 28, no. 11, pp. 2631-2654, Nov. 1992.

6. A. Szilagyi, A. Hordvik and H. Schlossberg, "A Quasi-Phase-Matching Technique for Efficient Optical Mixing and Frequency Doubling," *J. Appl. Phys.*, vol. 47, no. 5, pp. 2025-2032, May 1976.

7. D. E. Thompson, J. D. McMullen and D. B. Anderson, "Second-Harmonic Generation in GaAs "Stack of Plates" Using High-Power CO_2 Laser Radiation," *Appl. Phys. Lett.*, vol. 29, no. 2, pp. 113-115, Jul. 1976.

8. M. S. Piltch, C. D. Cantrell and R. C. Sze, "Infrared Second Harmonic Generation in Nonbirefringent Cadmium Telluride," *J. Appl. Phys.*, vol. 47, pp. 3514-3517, 1976.

9. L. A. Gordon, et al., "Diffusion Bonded Gallium Arsenide Stack of Plates for Quasi Phase Matched Second Harmonic Generation of a Carbon Dioxide Laser," in proceedings CLEO postdeadline, Optical Society of America, Baltimore, MD, May 1993.

10. L. A. Gordon, et al., "Diffusion Bonded Stacked GaAs for Quasi-Phase-Matched Second Harmonic Generation of a Carbon Dioxide Laser," *Electron. Lett.*, vol. 29, no. 22, pp. 1942-1943, Oct. 1993.

11. K. C. Rustagi, S. C. Mehendale and S. Meenakshi, "Optical Frequency Conversion in Quasi-Phase-Matched Stacks of Nonlinear Crystals," *IEEE J. Quantum Electron.*, vol. QE-18, no. 6, pp. 1029-1041, Jun. 1982.

12. M. J. Angell, et al., "Orientation Patterning of II-VI Semiconductor Films for Quasi-phasematched Nonlinear Devices," in proceedings Integrated Photonics Research, vol. 10, pp. 472-474, Optical Society of America, Palm Springs, CA, March 1993.

13. H. Mao, F. Fu, B. Wu and C. Chen, "Noncritical Quasiphase-Matched Second Harmonic Generation in LiB_2O_5 Crystal at Room Temperature," *Appl. Phys. Lett.*, vol. 61, no. 10, pp. 1148-1150, Sep. 1992.

14. D. A. Roberts, "Simplified Characterization of Uniaxial and Biaxial Nonlinear Optical Crystals: A Plea for Standardization of Nomenclature and Conventions," *IEEE J. Quantum Electron.*, vol. 28, no. 10, pp. 2057-2074, Oct. 1992.

15. S. Singh, "Nonlinear Optical Materials," in Handbook of Laser Science and Technology, ed. M. J. Weber, vol. 3, pp. 3-228, CRC, Boca Raton, FL, 1986.

16. P. Klocek, Handbook of Infrared Optical Materials, Marcel Dekker, Inc., New York, NY, 1991.

17. S. K. Kurtz, J. Jerphagnon and M. M. Choy, "Nonlinear Dielectric Susceptibilities," in Elastic, Piezoelectric, Pyroelectric, Piezooptic, Electrooptic Crystals, and Nonlinear Dielectric Susceptibilities of Crystals, ed. K. H. Hellwege, vol. 11, pp. 671-743, Landolt-Bornstein: Springer-Verlag, New York, 1979.

18. A. N. Pithkin and A. D. Yas'kov, "Dispersion of the Refractive Index of Semiconductors with Diamond Zinc-blende Structures," *Sov. Phys. Semicond.*, vol. 12, no. 6, pp. 622-626, Jun. 1978.

19. A. Yamada, M. Oasa, H. Nagabuchi and M. Kawashima, "Direct adhesion of single-crystal GaAs wafers," *Material Lett.*, vol. 6, no. 5.6, pp. 167-169, Mar. 1988.

20. Z. L. Liau and D. E. Mull, "Wafer Fusion: A Novel Technique for Optoelectronic Device Fabrication and Monolithic Integration," *Appl. Phys. Lett.*, vol. 56, no. 8, pp. 737-739, Feb. 1990.

21. Y. O. Lo, R. Bhat, D. M. Hwang, M. A. Koza and T. P. Lee, "Bonding by Atomic Rearrangement of InP/InGaAsP 1.5 μm Wavelength Lasers on GaAs Substrates," *Appl. Phys. Lett.*, vol. 58, no. 18, pp. 1961-1963, May 1991.

22. J. J. Dudley, et al., "144° C operation of 1.3μm InGaAsP vertical cavity lasers GaAs substrates," *Appl. Phys. Lett.*, vol. 61, no. 26, pp. 3095-3097, Dec. 1992.

23. Y. H. Lo, R. Bhat, D. M. Hwang, C. Chua and C. H. Lin, "Semiconductor lasers on Si substrates using the technology of bonding by atomic rearrangement," *Appl. Phys. Lett.*, vol. 62, no. 10, pp. 1038-1040, Mar. 1993.

24. R. J. Ram, et al., "Analysis of wafer fusing for 1.3μm vertical cavity surface emitting lasers," *Appl. Phys. Lett.*, vol. 62, no. 20, pp. 2474-2476, May 1993.

25. H. C. Lee, P. A. Brownlie, H. E. Meissner and E. C. Rea, "Diffusion Bonded Composites of YAG Single Crystals," in proceedings SPIE, vol. 1624, pp. 2-10, SPIE, Dec. 1991.

26. H. Tajima, M. Moriyama, N. Tadokoro, H. Hara and T. Mochizuki, "Performance of Composite Glass Slab Laser," *IEEE J. Quantum Electron.*, vol. 28, no. 6, pp. 1562-1569, Jun. 1992.

27. C. R. Barrett, W. D. Nix and A. S. Tetelman, The Principles of Engineering Materials, chap. 5-8, pp. 144-292, Prentice-Hall, Inc., Englewood Cliffs, NJ, 1973.

28. S. J. Brosnan and R. L. Byer, "Optical Parametric Oscillator Threshold and Linewidth Studies," *IEEE J. Quantum Electron.*, vol. 15, no. 6, pp. 415-431, 1979.

DIFFUSION BONDING OF GaAs WAFERS FOR NONLINEAR OPTICS APPLICATIONS

D. Zheng, L.A.Gordon, R.C.Eckardt,
M.M. Fejer and R.L. Byer
Edward L. Ginzton Laboratory
Stanford University, CA 94305

Diffusion-bonded stacked (DBS) periodic structures can create a new family of nonlinear optics crystals with spatially patterned nonlinear properties, while the bonding process preserves the optical and mechanical properties of the bulk materials. GaAs devices up to 20 layers were diffusion bonded and characterized. Optical loss was from interfacial voids and gaps at shorter wavelengths, and from processing induced p-type free carrier absorption at longer wavelengths.

INTRODUCTION

Laser sources in the spectral range between 1 μm and 10 μm have wide applications in spectroscopy, remote sensing and military countermeasures. However, currently available high-power lasers have output wavelengths around 1 μm (rare earth doped crystals) and at 10 μm (CO_2 laser). One way to generate laser radiation at mid-IR wavelengths is to extend present mature laser technology to these wavelengths by nonlinear optical frequency conversion. Unfortunately, existing infra-red nonlinear crystals are difficult to grow, have poor thermal properties, and are expensive.

GaAs has a large nonlinear coefficient, good optical transmission between 1 μm and 12 μm, and high optical damage threshold for high power applications. It has good chemical stability, good mechanical properties, and has a well developed growth technology. However, single crystal GaAs cannot be used directly for nonlinear frequency conversion because the interacting waves cannot be phasematched, i.e., there is no way to compensate for the wavelength dependence of the refractive indices (dispersion). In Figure 1(a), second harmonic generation (SHG) is shown as a function of length of crystal for a non-phasematched interaction. The fundamental wave has a different phase velocity from the second harmonic wave, due to dispersion. As the two interacting waves propagate through the crystal, the phase difference increases, and the conversion efficiency decreases. One coherence length into the crystal, the two waves are π out of phase, and the second harmonic wave starts converting back to the fundamental wave.

Changing sign of nonlinearity every coherence length allows growth of the second harmonic power (figure 1(b)). Sign of nonlinearity changes in $\bar{4}3m$ crystals with 180° rotation around $[1\,\bar{1}0]$. Stack of plates, each one coherence length thick, produces quasi-phasematching (QPM) structure. SHG using QPM interactions was first demonstrated in GaAs in 1976[1][2]. Plates were polished to one coherence length (106 μm for SHG of

10.6 μm radiation), and aligned at Brewster's angle. Enhanced conversion efficiency was measured; however, alignment was tedious and there were serious optical losses due to the many air-GaAs interfaces.

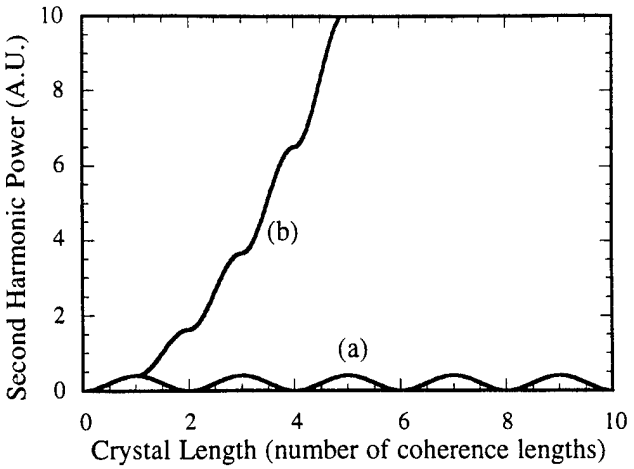

Figure 1. Theoretical second harmonic power as a function of crystal length
(a) Not phasematched interaction (b) Quasi-phasematched interaction

Direct material bonding of semiconductors has been used as an alternative to heteroepitaxy in electronic and optoelectronic devices[3-5]. While most work has been done with silicon, optoelectronic devices have been fabricated in the III-V semiconductors using various bonding techniques[6-8]. We have used direct material bonding to produce a DBS structure of GaAs plates for QPM interactions with reduced optical loss[9][10]. Figure 2 shows a schematic of a diffusion bonded crystal that can be used for frequency doubling a CO_2 laser radiation. Adjacent plates are rotated 180° to change the sign of the nonlinear coefficient. Commercial applications will require bonded stacks of 50 to 100 GaAs plates; therefore, loss introduced by bonding must be lower than 0.2% per layer for efficient frequency conversion. We report on our current work to understand and reduce processing-dependent losses.

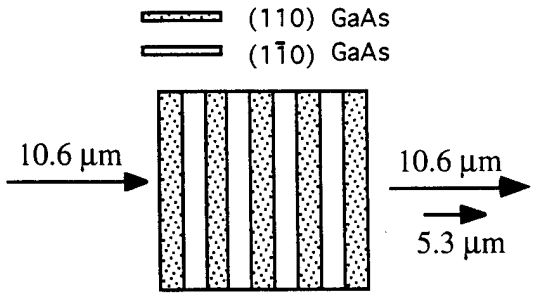

Figure 2. Diffusion-bonded stacked (DBS) GaAs for frequency doubling of 10.6 μm CO_2 radiation

PROCESSING

320 μm-thick {110} semi-insulating GaAs wafers were diced into 1 cm squares, which were cleaned and assembled in a cleanroom. The pieces were cleaned with hot detergent and de-ionized water, followed by degreasing baths of trichloroethane, acetone and methanol. The squares were then etched in NH_4OH for 15 min. After rinsing in flowing de-ionized water for 5 min, they were assembled by stacking alternating (110) and $(1\bar{1}0)$ GaAs plates under de-ionized water to reduce particle contamination at interfaces. The wafers were then placed into the bonding furnace shown in figure 3.

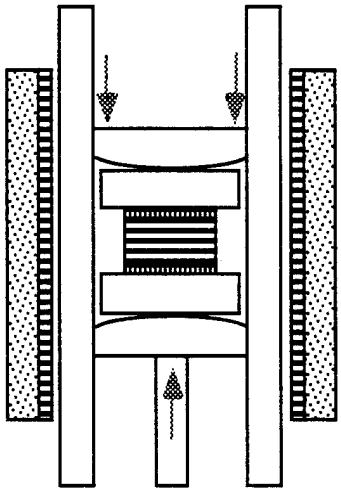

Figure 3. Schematic of the furnace used for bonding

The vertical furnace has two slightly radiused outer pressure plates to apply uniform pressure up to 10^7 N/m^2 (100 kg/cm^2). Pressure is applied by a pneumatic piston from outside the furnace, permitting variation at any time during the process. The furnace can maintain sample temperatures of up to 1000°C.

The wafers were bonded at temperatures ranging from 700°C to 975°C under a pressure up to 20 kg/cm^2 in ~10% H_2 + N_2 atmosphere. The samples remained at high temperature for 2 to 9 hours.

CHARACTERIZATION

Usually during polishing, the two sides of the wafer will develop slightly different surface qualities, therefore, during the process development, three pieces were bonded together each run to test bonding of both sides. After bonding, the samples were cleaved and large sections of the interfaces observed under an optical microscope. Voids at interfaces were observed to be less than 0.5 μm in diameter. Interfacial gaps less than 0.2 μm wide millimeters long occurred occasionally. Optical transmission was measured with a

Perkin-Elmer Lambda-9 spectrophotometer and a Bio-Rad FTS-40 FTIR. SEM and TEM were also use to characterize the interfaces. TEM indicates that bonding disrupts only a couple of atomic layers on each side of the interface.

RESULTS

The optical transmission spectrum of a 20 layer DBS GaAs is compared to that of an unprocessed single GaAs wafer in figure 4. Scattering from voids at interfaces can explain the loss at wavelengths between 1 μm and 2 μm, while gaps at interfaces may contribute to loss between 2 μm and 3 μm, however loss at wavelengths longer than 4 μm cannot be explained by either of these mechanisms.

Figure 5 shows transmission of a single wafer of GaAs annealed at 700°C to 975°C. Longer-wavelength-loss of single GaAs wafers increases as a function of annealing temperature. This loss at longer wavelengths is due to bulk absorption. Hall measurements show that semi-insulating wafers become p-type doped after annealing at 834°C, with a carrier concentration around $10^{16}/cm^3$. This is confirmed by the similarity of the loss spectrum to that of p-type free carrier absorption. The semi-insulating to p-type conversion has been reported previously[11-15] and is dependent on defect density as a function of temperature. It also depends on trace doping and the thermal history of the wafers. The annealing-induced loss is significantly reduced at 700°C.

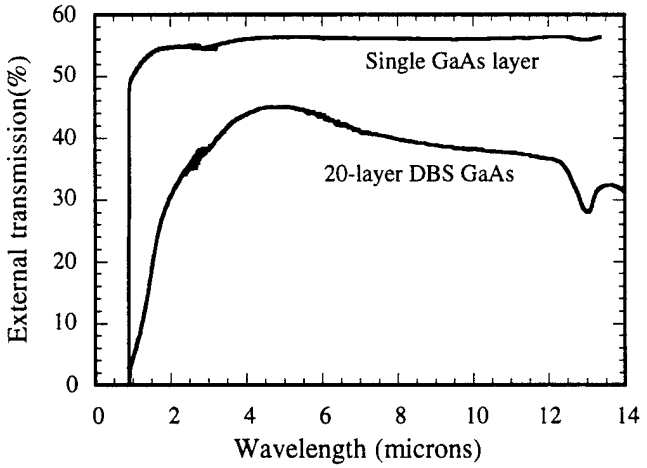

Figure 4. Transmission spectra of a 20-layer diffusion bonded stack (bonded at 834°C) and a single GaAs layer for reference

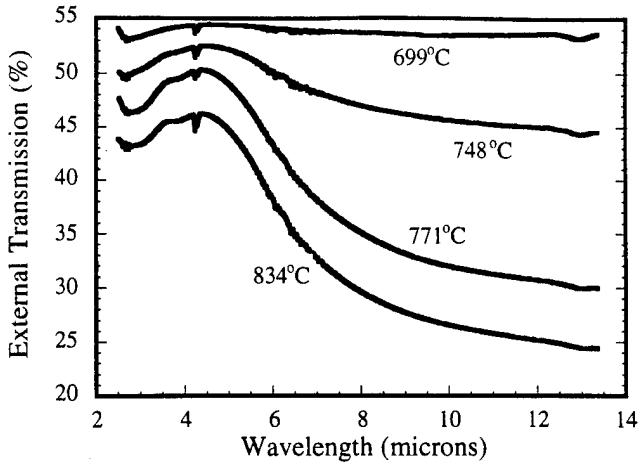

Figure 5. Transmission of a single GaAs wafer annealed at different temperatures

SUMMARY

In summary, we bonded multiple GaAs layers for nonlinear optics applications. Loss is from interfacial voids and gaps at shorter wavelengths, and processing induced p-type free carrier absorption at longer wavelengths. Induced loss is significantly lower for annealing at 700°C. To further reduce loss of DBS GaAs, we are currently using etching instead of dicing to cut wafers into small pieces for bonding so as to avoid contamination by the saw lubricant and debris, and lowering bonding temperature to avoid p-type conversion.

ACKNOWLEDGMENTS

The authors would like to thank Guoying Ding for the Hall measurements. This work is supported by ARPA through center for nonlinear optics materials.

REFERENCES

[1] A. Szilagyi, A. Hordvik and H. Schlossberg, "A Quasi-Phase-Matching Technique for Efficient Optical Mixing and Frequency Doubling," J. Appl. Phys. **47,** p. 2025-2032 (1976).

[2] D. E. Thompson, J. D. McMullen and D. B. Anderson, "Second-Harmonic Generation in GaAs "Stack of Plates" Using High-Power CO_2 Laser Radiation," Appl. Phys. Lett. **29,** p. 113-115 (1976).

[3] A. Yamada, M. Oasa, H. Nagabuchi and M. Kawashima, "Direct adhesion of single-crystal GaAs wafers," Material Lett. **6,** p. 167-169 (1988).

[4] W. P. Maszara, G. Goetz, A. Caviglia and J. B. McKitterick, "Bonding of silicon wafers for silicon-on-insulator," J. Appl. Phys. **64,** p. 4943-4950 (1988).

[5] V. Lehmann, K. Mitani, R. Stengl, T. Mii and U. Gösele, "Bubble-Free Wafer Bonding of GaAs and InP on Silicon in a Microcleanroom," Jap. J. Appl. Phys. **28,** p. L2141-L2143 (1989).

[6] Y. O. Lo, R. Bhat, D. M. Hwang, M. A. Koza and T. P. Lee, "Bonding by Atomic Rearrangement of InP/InGaAsP 1.5 μm Wavelength Lasers on GaAs Substrates," Appl. Phys. Lett. **58,** p. 1961-1963 (1991).

[7] Z. L. Liau and D. E. Mull, "Wafer Fusion: A Novel Technique for Optoelectronic Device Fabrication and Monolithic Integration," Appl. Phys. Lett. **56,** p. 737-739 (1990).

[8] R. J. Ram, L. Yang, K. Nauka, Y. M. Houng, M. Ludowise, D. E. Mars, J. J. Dudley and S. Y. Wang, "Analysis of wafer fusing for 1.3μm vertical cavity surface emitting lasers," Appl. Phys. Lett. **62,** p. 2474-2476 (1993).

[9] L. A. Gordon, G. L. Woods, R. C. Eckardt, R. K. Route, R. S. Feigelson, M. M. Fejer and R. L. Byer, "Diffusion Bonded Stacked GaAs for Quasi-Phase-Matched Second Harmonic Generation of a Carbon Dioxide Laser," Electron. Lett. **29,** p. 1942-1943 (1993).

[10] L. A. Gordon, R. C. Eckardt and R. L. Byer, "Investigations of Diffusion-Bonded Stacked GaAs for Infrared Quasi-Phasematched Parametric Oscillation," ed. (SPIE, Los Angeles, CA, 1994) p. 316-26

[11] C. H. Kang, J. Lagowski and H. C. Gatos, "Characteristics of GaAs with Inverted Thermal Conversion," J. Appl. Phys. **62,** p. 3482-3485 (1987).

[12] P. Kidd, D. J. Stirland and G. R. Booker, "Observations of Individual Precipitate particles Associated with the Same Dislocations Within a Bulk In-Doped GaAs Specimen Before and After Furnace Annealing," Mat. Letters **9,** p. 521-525 (1990).

[13] J. Lagowski, H. C. Gatos, C. H. Kang, K. Y. Skowronski, K. Y. Ko and D. G. Lin, "Inverted Thermal Conversion-GaAs, a New Alternative Material for Integrated Circuits," Appl. Phys. Lett. **49,** p. 892-894 (1986).

[14] D. C. Look, P. W. Yu, W. M. Theis, W. Ford, G. Mathur, J. R. Sizelove, D. H. Lee and S. S. Li, "semiconducting/ Semi-Insulating Reversibility in Bulk GaAs," Appl. Phys. Lett. **49,** p. 1083-1085 (1986).

[15] O. Oda, H. Yamamoto, M. Seiwa, G. Kano, T. Inoue, M. Mori, H. Shimakura and M. Oyake, "Defects in and Device Properties of Semi-Insulating GaAs," Semicond. Sci. Technol. **7,** p. A215-A223 (1992).

Progress in Reducing Loss of Diffusion Bonded Stacked GaAs for Mid Infra-Red Generation

D. Zheng, L. A. Gordon, Y. S. Wu, R. C. Eckardt,
M. M. Fejer, R. L. Byer and R. S. Feigelson

Edward L. Ginzton Laboratory
Stanford University, CA 94305
Tel. (415) 723-1718
Fax. (415) 723-2666

Mid infra-red (IR) sources between 1 μm and 10 μm have wide applications in spectroscopy, remote sensing and military countermeasures. Established nonlinear IR crystals such as $AgGaSe_2$, and $AgGaS_2$ have poor thermal properties, and low damage thresholds. $ZnGeP_2$ appears promising for high power applications, but its growth technology is still being developed, and crystals are expensive. In comparison, GaAs has a large nonlinear coefficient, good optical transmission between 1 μm and 12 μm, and high optical damage threshold. It also has good chemical stability, good mechanical properties, and a well developed growth technology. Unfortunately, single crystal GaAs is linearly isotropic; therefore, nonlinear interactions cannot be birefringently phase-matched. However, the interacting waves can be quasi-phasematched (QPM) by periodically modulating the nonlinear coefficient in a stack of rotated plates[1,2]. By diffusion bonding individual plates together, we can minimize scattering and reflection losses at the air-GaAs interfaces. Preliminary diffusion-bonded-stacked (DBS) GaAs devices demonstrated close to theoretical conversion efficiency[3,4], but had high transmission losses. We report improved processing, leading to a significant reduction in the transmission loss to less than 0.2% per layer at 5 μm.

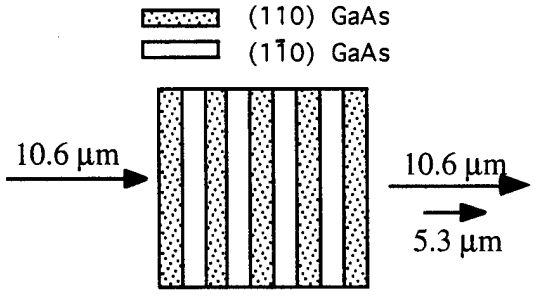

Figure 1. Diffusion-bonded stacked (DBS) GaAs for quasi-phasematched second harmonic generation of 10.6 μm CO_2 radiation

{110} wafers were chosen to provide the maximum effective nonlinear coefficient for propagation normal to the input face. Each plate is three coherence lengths thick, with adjacent plates rotated 180° to change the sign of the nonlinear coefficient. Stacks are heated to 700-975°C under pressure to achieve diffusion bonding at the interfaces. Figure 1 illustrates second harmonic generation in DBS GaAs. A range of applications become practical for stacks with less than 0.1% additional loss per interface. Losses from both the interfaces and bulk material contribute to the total loss of DBS

GaAs. Incomplete bonding between surfaces leaves microscopic voids and gaps. Scattering due to these irregularities is the dominant loss mechanism for wavelengths less then 3 μm.

Recently, we have discovered that the bulk material undergoes a conversion during the annealing process[5]. Loss in DBS GaAs at longer-wavelengths is a result of bulk p-type free carrier absorption. Semi-insulating wafers can convert to p-type during the annealing step, dependent on soak temperatures and times, and quenching rates[6]. Conversion is also affected by thermal history and composition of wafers; it is, therefore, supplier specific. Our semi-insulating wafers converted to p-type after annealing at 834°C, with a hole concentration of around $10^{16}/cm^3$. By annealing individual wafers, we found the longer-wavelength loss increased with processing temperatures from 700°C to 834°C, as shown in figure 2. The annealing-induced loss is significantly reduced at 700°C.

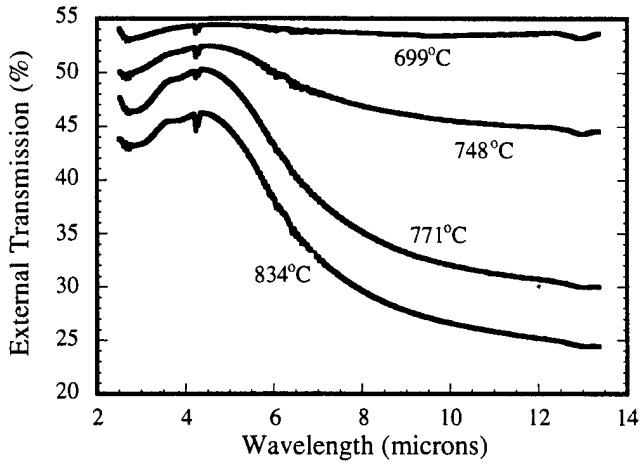

Figure 2. Transmission of a single 320-μm thick GaAs wafers annealed at different temperatures

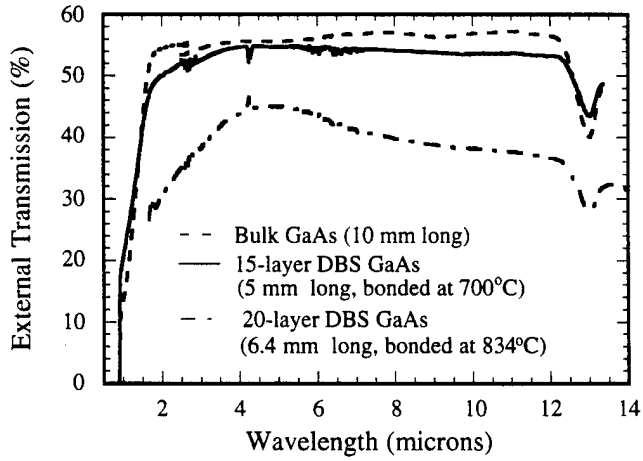

Figure 3. Comparison of the transmission spectra of the 15-layer DBS GaAs (bonded at 700°C), with the 20-layer DBS GaAs (bonded at 834°C), and a 1 cm long unprocessed bulk GaAs crystal

Figure 3 compares the optical transmission of two DBS devices bonded at different temperatures with the transmission of the bulk unprocessed GaAs. All the GaAs is from the same boule. The 20-layer DBS GaAs device, bonded earlier at 834°C, shows transmission is significantly reduced; at 5 μm the internal loss is 0.3 cm^{-1}, corresponding to 1.5% per layer. The recent 15-layer DBS device was bonded at 700°C. Its transmission at wavelengths longer than 3 μm is relatively flat, with a total internal loss of about 0.04 cm^{-1} at 5 μm, corresponding to less than 0.2% per layer. It appears that there could still be some transformation from semi-insulating to p-type doped material even at processing temperatures of 700°C. We should be able to further improve the optical transmission by lowering the temperature again, provided that we are still able to bond the wafers at the lowered temperatures, by requiring specific compositions from manufacturers, or by implementing a post-bonding annealing step. GaAs manufacturers employ multiple annealing steps to ensure high quality, uniformly semi-insulating crystals. Using similar processing techniques, we can regain high quality semi-insulating material.

In summary, a nonlinear frequency conversion device requires low loss. At higher temperatures, semi-insulating GaAs transforms into p-type, resulting in longer-wavelength absorption. By bonding at lower temperatures, we have reduced the loss to less than 0.2% per layer at 5 μm. However, some of the remaining loss is still due to p-type free carrier absorption. We plan to fabricate longer devices and demonstrate efficient second harmonic generation of high power CO_2 laser radiation.

REFERENCES

[1] A. Szilagyi, A. Hordvik and H. Schlossberg, "A Quasi-Phase-Matching Technique for Efficient Optical Mixing and Frequency Doubling," J. Appl. Phys. **47,** p. 2025-2032 (1976).

[2] D. E. Thompson, J. D. McMullen and D. B. Anderson, "Second-Harmonic Generation in GaAs "Stack of Plates" Using High-Power CO_2 Laser Radiation," Appl. Phys. Lett. **29,** p. 113-115 (1976).

[3] L. A. Gordon, G. L. Woods, R. C. Eckardt, R. K. Route, R. S. Feigelson, M. M. Fejer and R. L. Byer, "Diffusion Bonded Stacked GaAs for Quasi-Phase-Matched Second Harmonic Generation of a Carbon Dioxide Laser," Electron. Lett. **29,** p. 1942-1943 (1993).

[4] L. A. Gordon, D. Zheng, Y. C. Wu, R. C. Eckardt, R. K. Route, R. S. Feigelson, M. M. Fejer and R. L. Byer, "Diffusion Bonded Stacked Materials for High Peak and Average Power IR Application", invited paper CLEO Pacific Rim, July 1995

[5] D. Zheng, L. A. Gordon, R. C. Eckardt, M. M. Fejer and R. L. Byer, "Diffusion Bonding of GaAs Wafers for Nonlinear Optics Applications," Proceedings of the 189th Electrochemical Society Meeting, to be published.

[6] D. C. Look, P. W. Yu, W. M. Theis, W. Ford, G. Mathur, J. R. Sizelove, D. H. Lee and S. S. Li, "semiconducting/ Semi-Insulating Reversibility in Bulk GaAs," Appl. Phys. Lett. **49,** p. 1083-1085 (1986).

REPORT DOCUMENT PAGE

Standard form 298 (Rev. 2-89) facsimile

1. AGENCY USE ONLY *(Leave blank)*

2. REPORT DATE
April 1996

3. REPORT TYPE AND DATES COVERED
Final Technical Report

4. TITLE AND SUBTITLE
Diffusion-Bonded Nonlinear Materials for Practical Quasi-Phasematched Mid-IR Devices

5. FUNDING NUMBERS
N00014-94-1-0426

6. AUTHORS
L. A. Gordon, Z. Dong, S. Wu, R. C. Eckardt, R. K. Route, R. S. Feigelson and R. L. Byer

7. PERFORMING ORGANIZATION NAME(S) AND ADDRESSES
Edward L. Ginzton Laboratory
Stanford University
Stanford, CA 94305-4085

8. PERFORMING ORGANIZATION REPORT NUMBER
Ginzton Report No. 5409

9. SPONSORING / MONITORING AGENCY NAME(S) AND ADDRESS(ES)
Office of Naval Research
Ballston Tower One
800 North Quincy Street
Arlington, VA 22217-5660

10. SPONSORING / MONITORING AGENCY REPORT NUMBER

11. SUPPLEMENTARY NOTES
The view, opinions and/or findings contained in this report are those of the author(s) and should not be construed as an official Department of the Navy position, policy, or decision, unless so designated by other documentation.

12a. DISTRIBUTION / AVAILABILITY STATEMENT
Approved for public release; distribution unlimited.

12b. DISTRIBUTION CODE

13. ABSTRACT ***(Maximum 200 words)***

This report summarizes research on the application of diffusion-bonded GaAs for high power quasi-phasematched nonlinear frequency conversion in the infrared (IR). Research focused on development of material processing methods. Microstructural, microchemical and optical characterization techniques were employed to analyze the nature of defects found at the wafer interfaces, and within the bulk material; strategies for minimizing them were developed. The resulting advances in processing technology reduced mid-IR optical losses in diffusion-bonded GaAs stacks by over an order of magnitude, to less than 0.2% per interface. This is within the range required to make practical pulsed nonlinear infrared devices such as CO_2 doublers. Further reductions in optical losses, required for high average power cw IR applications, appear possible.

14. SUBJECT TERMS
Diffusion-bonding, diffusion-bonded GaAs, quasi-phasematching, IR devices, GaAs, nonlinear optical materials

15. NUMBER OF PAGES
62

16. PRICE CODE

17. SECURITY CLASSIFICATION OF REPORT	18. SECURITY CLASSIFICATION OF THIS PAGE	19. SECURITY CLASSIFICATION OF ABSTRACT	20. LIMITATION OF ABSTRACT
UNCLASSIFIED	UNCLASSIFIED	UNCLASSIFIED	UL